Premoli Silva, I., Haggerty, J., Rack, F., et al., 1993
*Proceedings of the Ocean Drilling Program, Initial Reports*, Vol. 144

# 8. SITE 877[1]

Shipboard Scientific Party[2]

## HOLE 877A

**Date occupied:** 19 June 1992

**Date departed:** 21 June 1992

**Time on hole:** 1.84 days, 20 hr, 10 min

**Position:** 12°01.146′N, 164°55.326′E

**Bottom felt (rig floor, m; drill-pipe measurement):** 1366.0

**Distance between rig floor and sea level (m):** 11.2

**Water depth (drill-pipe measurement from sea level, m):** 1354.8

**Total depth (rig floor, m):** 1556.5

**Penetration (m):** 190.5

**Number of cores (including cores with no recovery):** 20

**Total length of cored section (m):** 190.40

**Total core recovered (m):** 25.23

**Core recovery (%):** 13.3

**Oldest sediment cored:**
Depth (mbsf): 189.0
Nature: clay

**Hard rock:**
Depth (mbsf): 189.0
Nature: basalt

**Basement**
Depth (mbsf): 189.0
Nature: basalt

**Principal results:** Site 877 is located at 12°01.14′N, 164°55.30′E, in 1355 m water depth, on the northeastern rim of Wodejebato Guyot, in the Ralik Chain of the northern Marshall Islands. Site 877 is located on the inner perimeter ridge, 0.7 km northeast of Site 874 (which is located on the same bathymetric ridge), and 1.2 km west-southwest of Site 876 (which is located on the outer ridge). Site 874 is located on the seaward crest of the ridge, whereas Site 877 is slightly more centrally located on the seaward summit of the ridge. Coring began at Site 877 on 19 June 1992 and was completed on 21 June, after 1.84 days. A single hole was drilled; recovery was 13.2%, including one core with zero recovery. After we obtained our drilling objectives in Hole 877A, we departed Site 877 on 21 June 1992 and moved to Hole 801C.

The objectives of drilling at this location were (1) to verify the areal extent of reef facies on the inner perimeter ridge and their distribution in time; (2) to correlate the facies from the outer perimeter ridge; (3) to compare the carbonate sequences across the margin of the guyot; (4) to correlate among sites using the seismic records that traverse both the inner and outer perimeter ridges; and (5) to interpret the subsidence history of the platform relative to sea-level fluctuations.

Four lithologic units were recognized at Site 877, using a combination of visual core descriptions and smear slide and thin-section data. The age of these units was determined from the identification of larger benthic foraminifers, macrofossils (rudists), and calcareous nannofossils. The following lithologic units were recognized:

Unit I (0–0.2 mbsf) consists of manganese-encrusted and phosphatized limestone of middle Eocene age. The host substrate is composed of Maastrichtian shallow-water packstone with cavities infilled with partially phosphatized pelagic sediments of late middle Eocene, early Eocene, and late Paleocene age.

Unit II (0.2–183 mbsf) consists predominantly of white to light brown and pinkish white Maastrichtian grainstones. Also present are Maastrichtian boundstone, packstone, wackestone, and floatstone. The average carbonate content is 98%. Major components include rudists (caprinids and radiolitids), red algae (corallinaceans, squamariaceans), benthic foraminifers (mostly larger foraminifers and miliolids), common mollusk molds, corals, stromatoporoids, and few echinoids. Unit II is divided into five subunits on the basis of depositional texture, variations in skeletal constituents, and color. Estimated porosity ranges mainly from 2% to 25%. Porosity is mostly moldic (after caprinid shells, other bivalves, or gastropods) and interparticle to vuggy (few solution-enlarged interparticle pores). Solution cavities in the upper 20 cm of the unit contain pelagic geopetal sediments of Maastrichtian, late Paleocene, and early Eocene age. Lithoclasts containing larger foraminifers occur at the base of the platform sequence and indicate reworking in moderately high-energy conditions. The basal portion of Site 877 correlates with that of Site 874. Unit II is thicker at Site 877 than at Site 874; more reef development is present at Site 877.

Unit III (183–186 mbsf) consists of black clay, argillaceous limestone, peat, reddish brown clay, and claystone breccia of late Campanian to indeterminate age. Argillaceous limestone contains thin-shelled mollusk fragments, benthic foraminifers, and calcareous nannofossils of late Campanian age associated with reworked Cenomanian species. Black clay is rich in plant remains and common pyrite; total organic carbon (TOC) averages 1.48% and sulfur averages 8.72%. In the peat layer, TOC averages 12.45% (maximum = 37%), whereas sulfur content averages 23.55% (maximum = 25%). Root molds are present in the clays beneath the peat. Downhole, the organic carbon and sulfur contents of the clay and claystone decrease, as the features of a volcanic breccia become progressively more preserved. A clast of basalt is present in the lower part of the unit.

Unit IV (186–190.5 msbf) consists of basaltic breccia with clasts of vesicular, glassy, alkalic basalt containing xenocrysts of plagioclase and clinopyroxene. The clasts contain irregularly shaped vesicles. The matrix of the breccia is composed of fragmented basaltic material that has been extensively replaced by green and brown clay. Thin, anastomosing subhorizontal calcite veins replace almost 50% of the breccia. Two discrete samples of basalt were demagnetized and their magnetic properties measured. The samples had well-defined characteristic magnetization yielding positive inclinations (+8.9° and +14.2°), similar to samples from elsewhere on the guyot. These positive inclinations possibly represent a reversed polarity magnetization acquired in the Southern Hemisphere. The results from Site 877, combined with data from all the sites on Wodejebato Guyot, yield a paleolatitude near 10°S.

## BACKGROUND AND OBJECTIVES

For a discussion of the geologic history of Wodejebato Guyot and previous studies, see the "Background and Objectives" section for Site 873 (this volume).

Site 877 is located on the northeastern rim of Wodejebato Guyot in the northern Marshall Islands. Site 877 is located on the inner perimeter ridge of the guyot, about 0.7 km north of Site 874. A primary objective of Site 877 was to verify the areal extent of

[1] Premoli Silva, I., Haggerty, J., Rack, F., et al., 1993. *Proc. ODP, Init. Repts.*, 144: College Station, TX (Ocean Drilling Program).

[2] Shipboard Scientific Party is as given in the list of participants preceding the contents.

reef facies on the inner perimeter ridge and their distribution in time through comparisons with Site 874.

The position of Site 877 is only 1.2 km southwest of Site 876. These sites are paired: one on the outer perimeter ridge and one on the inner perimeter ridge. With this configuration of the drill sites, the carbonate facies across the margin of the guyot can be compared. Another objective of Site 877 was to correlate among sites using the seismic records that traverse both the inner and outer perimeter ridges. This can then be used to interpret the subsidence history of the atoll relative to sea-level fluctuations.

Drilling at Site 877 was very successful. The primary objectives associated with this site are addressed with the preliminary shipboard studies and additional shore-based studies.

## OPERATIONS

### Site 877—Wodejebato Guyot, Inner Perimeter Ridge

After completion of Hole 876A and while the pipe trip was in progress, the transit to Site 877 was accomplished in dynamic positioning (DP) mode. Bathymetry and sediment cover were monitored using the record from the 3.5-kHz echo sounder to ensure that the swale was crossed between the inner and outer perimeter ridges. The positioning beacon was recalled upon our departure from Site 876 and was redeployed at 0515L (L = local time) on 19 June 1992 for Site 877.

Site 877 is about 1.3 km to the southwest of Site 876. Site 877 was drilled on the inner perimeter ridge as a site paired with Site 876 on the outer perimeter ridge. The two sites are on a transect nearly perpendicular to the axes of the ridges and the upper flank of the guyot. These sites provide a comparison between the inner and outer ridges at adjacent positions on the northeastern rim of the guyot. At a depth of 1355 m below sea level, Site 877 was on a bathymetric high and 44 m shallower than Site 876. In addition, Site 877 is located 2.6 km to the northwest of Site 874 on the same inner perimeter ridge; both sites are located on the seaward summit of the ridge, but Site 877 is slightly inboard or more centrally located on the summit of the ridge than Site 874. A stratigraphic section similar to that recovered at Site 874 was expected.

### Hole 877A

The short, light "bare-rock," rotary-core-barrel (RCB) bottom-hole assembly (BHA) was readied, this time with a conventional RBI C-3 roller-cone core bit rather than a C-4 roller-cone core bit. The C-3 bit is designed for medium density formations; it has a slightly softer cutting structure, therefore, than bits used at previous RCB bare-rock spud sites. This change in operational strategy was an attempt to maximize the rate of penetration (ROP) in an uppermost section composed of manganese crust, hardground, and indurated limestone by using the very limited available BHA weight in a nearly bare-rock spud-in location.

The 3.5-kHz echo-sounder records had indicated 5–7 m of soft pelagic cover at the site, but only 1 m was found upon spudding the hole. The bit rotated for some time on the hard crust before it began to drill; over 1 hr was required to penetrate the first meter of limestone. Coring continued in hard limestone at a slow rate, with only minimal drill-collar weight and slow rotation. The ROP averaged only about 2½ m/hr for the first 50 m. Core recovery over the interval was about 21% (see Table 1) and was consistent with the observed inverse relationship between core recovery and the ROP.

Below 77 mbsf, boundstone and rudstone gave way to a less cemented grainstone containing more rubble. The poorly cemented grainstone was cored at rates up to 300 m/hr and core recovery was predictably minuscule. The grainstones became better cemented below about 150 mbsf, but core recovery rates remained at only about 4%.

**Table 1. Coring summary, Site 877.**

| Core no. | Date (June 1992) | Time (Z) | Depth (mbsf) | Cored (m) | Recovered (m) | Recovery (%) |
|---|---|---|---|---|---|---|
| 144-877A- | | | | | | |
| 1R | 19 | 0555 | 0–9.5 | 9.5 | 2.28 | 24.0 |
| 2R | 19 | 0940 | 9.5–19.0 | 9.5 | 0.58 | 6.1 |
| 3R | 19 | 1135 | 19.0–28.4 | 9.4 | 1.28 | 13.6 |
| 4R | 19 | 1655 | 28.4–38.0 | 9.6 | 3.00 | 31.2 |
| 5R | 19 | 2230 | 38.0–47.6 | 9.6 | 3.09 | 32.2 |
| 6R | 20 | 0115 | 47.6–57.3 | 9.7 | 1.27 | 13.1 |
| 7R | 20 | 0335 | 57.3–67.0 | 9.7 | 2.56 | 26.4 |
| 8R | 20 | 0525 | 67.0–76.6 | 9.6 | 0.54 | 5.6 |
| 9R | 20 | 0630 | 76.6–86.3 | 9.7 | 0.28 | 2.9 |
| 10R | 20 | 0730 | 86.3–96.0 | 9.7 | 0.20 | 2.1 |
| 11R | 20 | 0830 | 96.0–105.6 | 9.6 | 0 | 0 |
| 12R | 20 | 0930 | 105.7–115.3 | 9.6 | 0.21 | 2.2 |
| 13R | 20 | 1025 | 115.3–125.0 | 9.7 | 0.20 | 2.1 |
| 14R | 20 | 1125 | 125.0–134.6 | 9.6 | 2.16 | 22.5 |
| 15R | 20 | 1215 | 134.6–144.3 | 9.7 | 0.30 | 3.1 |
| 16R | 20 | 1325 | 144.3–153.9 | 9.6 | 0.50 | 5.2 |
| 17R | 20 | 1430 | 153.9–163.5 | 9.6 | 0.19 | 2.0 |
| 18R | 20 | 1545 | 163.5–173.2 | 9.7 | 0.58 | 6.0 |
| 19R | 20 | 1710 | 173.2–182.7 | 9.5 | 0.28 | 3.0 |
| 20R | 20 | 1900 | 182.7–190.5 | 7.8 | 5.73 | 73.4 |
| Coring totals | | | | 190.4 | 25.23 | 13.3 |

The ROP decreased somewhat at about 184 mbsf in Core 144-877A-20R, and hard drilling was encountered at about 189 mbsf. When the bit had reached 190.5 mbsf, the core was recovered to confirm that the basalt objective had been reached. The core barrel contained nearly 5 m of varicolored clay overlying about 1 m of altered basalt. As the scientific objectives in Hole 877A and at Wodejebato Guyot were complete, the drill string was recovered.

One final surprise remained at Hole 877A: as the bit was pulled into the bit-sized hole in the hard upper limestone, the hole became tight and it was necessary to pull to 90,000 lb over string weight to work the bit upward. About 30 min were required to ease the bit through a 20-m interval before the drag abated.

Average recovery at Hole 877A was 13.2%, including one core with no recovery. The *JOIDES Resolution* was underway to Site 801 by 1030L on 21 June 1992 and continued its transit to Site 801 on 22 June 1992.

## LITHOSTRATIGRAPHY

Site 877 is located on the inner perimeter ridge of northeastern Wodejebato Guyot. One hole was drilled at this site to a total depth of 190.5 mbsf using the RCB; core recovery was 13.2%.

Drilling results and lithologic units are summarized in a single lithostratigraphic framework (Fig. 1 and Table 2). Lithologic units are identified by such characteristics as color, carbonate and clay content, fossil and particle constituents, lithification, and sedimentary structures. The four major lithologies identified at this site are (1) manganese crust (Unit I, 0–0.03 mbsf); (2) rudist algal foraminifer limestone (Unit II, 0.03–182.9 mbsf); (3) clay, claystone, and claystone breccia (Unit III, 182.9–190.2 mbsf); and (4) volcanic breccia (Unit IV, 190.2–190.5 mbsf).

### Unit I

Interval: Section 144-877A-1R-1, 0–3 cm
Depth: 0–0.03 mbsf
Age: early and middle Eocene

Unit I consists of a 3-cm-thick, black (N2) manganese crust that cuts the underlying rock at apparent angles of 45° and 120°,

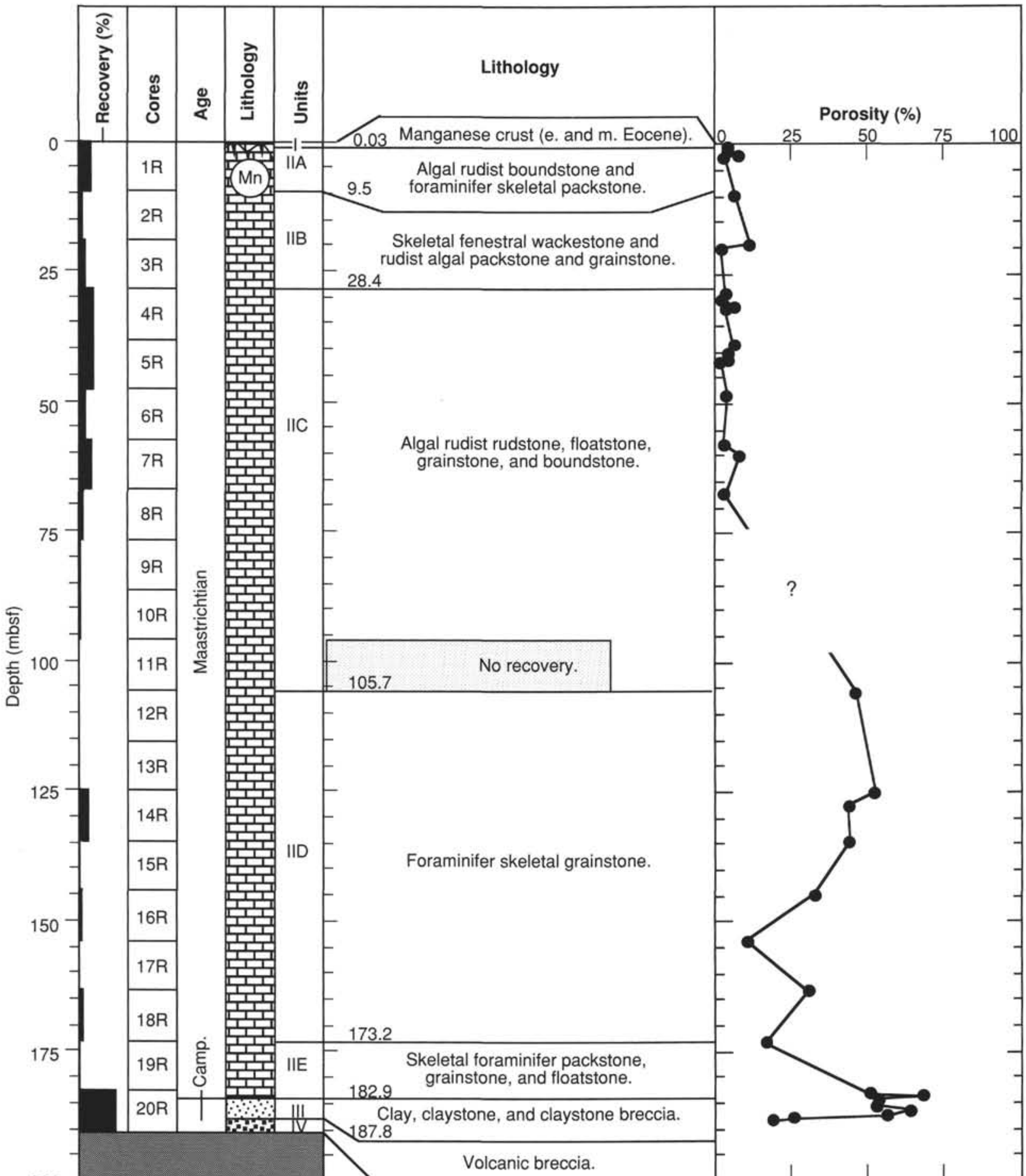

Figure 1. Lithostratigraphic summary and porosity values for Site 877.

as indicated by geopetal sediment fill. The crust is apparently featureless, except for lenses of white (10YR 8/1) pelagic limestone and white (10YR 8/2) wackestone (the host rock), which are centripetally replaced by botryoidal manganese dendrites 150 μm in diameter and impregnated locally by phosphate.

## Unit II

Interval: Section 144-877A-1R-1, 3 cm, through Core 144-877A-19R
Depths: 0.03–182.9 mbsf
Age: Maastrichtian

Unit II is comprised of 182.6 m of platform carbonates dominated by grainstone, but also including boundstone, packstone, wackestone, and floatstone. The color of the limestone ranges from white (10YR 8/2) and very pale brown (10YR 8/4, 10YR 7/3), to pale brown (10YR 6/3), to light gray (10YR 7/2) and pinkish white (5YR 8/2); brownish yellow with dusky red (2.5YR 3/2) and dark gray (2.5YR N4) patches are present at the base of the sequence.

Major components include rudists (caprinids and radiolitids), red algae (corallinaceans and squamariaceans), and benthic

**Table 2. Lithostratigraphic summary, Site 877.**

| Unit/subunit | Depth (mbsf) | Age | Cores | Thickness (m) | Lithology |
|---|---|---|---|---|---|
| Unit I | 0.0–0.03 | middle Eocene | 144-877A-1R-1, 0–3 cm | 0.03 | Manganese crust |
| Unit II | 0.03–182.9 | Maastrichtian | 144-877A-1R-1, 3 cm, through -19R | 182.60 | Platform carbonates |
| Subunit IIA | 0.03–9.5 | Maastrichtian | 144-877A-1R-1, 3 cm, through -1R | 9.47 | Skeletal packstone, rudstone, and boundstone |
| Subunit IIB | 9.5–28.4 | Maastrichtian | 144-877A-2R through -3R | 18.90 | Skeletal wackestone, packstone, and grainstone |
| Subunit IIC | 28.4–105.7 | Maastrichtian | 144-877A-4R through -11R | 77.30 | Skeletal grainstone, rudstone, floatstone, and boundstone |
| Subunit IID | 105.7–173.2 | Maastrichtian | 144-877A-12R through -18R | 67.50 | Skeletal grainstone and packstone |
| Subunit IIE | 173.2–182.9 | Maastrichtian | 144-877A-19R through -20R-1, 20 cm | 16.50 | Skeletal packstone and floatstone |
| Unit III | 182.9–187.8 | Campanian to ? | 144-877A-20R-1, 20 cm, to -20R-4, 110 cm | 4.90 | Clay and claystone |
| | 182.9–184.16 | Campanian to ? | 144-877A-20R-1, 20 cm, to -20R-2, 46 cm | 1.26 | Organic-rich clay |
| | 184.16–185.02 | ? | 144-877A-20R-2, 46 cm, to -20R-2, 132 cm | 0.86 | Clay |
| | 185.02–186.1 | ? | 144-877A-20R-2, 132 cm, to -20R-3, 90 cm | 1.08 | Claystone |
| | 186.1–187.8 | ? | 144-877A-20R-3, 90 cm, to -20R-4, 110 cm | 1.70 | Claystone breccia |
| Unit IV | 187.8–188.4 | ? | 144-877A-20R-4, 110–140 cm | 0.30 | Volcanic breccias |

foraminifers (mostly larger foraminifers and miliolids); mollusk molds (bivalves and gastropods), corals, and stromatoporoids are common; echinoids are few. This limestone also includes a rich assemblage of larger foraminifers including orbitoids, *Sulcoperculina, Asterorbis,* and *Omphalocyclus* (?), indicating a Maastrichtian age. The platform limestone contains few planktonic foraminifers of middle Maastrichtian age (e.g., Intervals 144-877A-7R-2, 109–120 cm; -18R-1, 25–28 cm; and -19R-1, 27–30 cm) (see "Biostratigraphy" section, this chapter).

At the top of the limestone, millimeter-sized vugs are filled by several generations of white (10YR 8/2) to light gray (10YR 7/1) isopachous calcite cements and very light brown (10YR 8/4) internal sediment. The internal sediment is a packstone formed either with fragments of red algae, bivalves, and benthic foraminifers, or with planktonic foraminifers. The assemblage of planktonic foraminifers is indicative of a middle Eocene age (see "Biostratigraphy" section, this chapter). A very pale brown (10YR 8/4 and 7/3) mudstone with planktonic foraminifers also fills some cavities within the Maastrichtian platform carbonates (e.g., Intervals 144-877A-1R-1, 3–24 cm; -1R-2, 90–95 cm; -2R-1, 6–20 cm; -3R-1, 9–11 cm; and -3R-1, 92–97 cm). Many of the void-filling limestones are stained yellow to brown (phosphate?); abundant black manganese micro-concretions (<0.25 mm) occur in the mudstone. The void fillings are mid-Maastrichtian, late Paleocene, and early Eocene in age (see "Biostratigraphy" section, this chapter).

Unit II is divided into five subunits on the basis of depositional texture, variations in skeletal constituents, and color. Relationships between measured porosity (see "Physical Properties" section, this chapter) and lithologic subunits are summarized in Figure 1. Porosity estimated visually was systematically lower than measured porosity.

In the interval from 0.03 to 182.9 mbsf, the recovery averaged 10.7%; recovery was nil between 96 and 105.7 mbsf (see "Operations" section, this chapter).

### *Subunit IIA*

Interval: Section 144-877A-1R-1, 3 cm, to -2R-1, 0 cm
Depths: 0.03–9.5 mbsf
Age: Maastrichtian

Subunit IIA consists of 9.47 m of foraminifer skeletal packstone, algal boundstone, and rudist rudstone. The color of the limestone is white (10YR 8/2) to very pale brown (10YR 8/4) and pinkish white (5YR 8/2). Recovery averaged 24% in this interval (see "Operations" section, this chapter). In Subunit IIA, calcium carbonate content averages 98% (see "Organic Geochemistry" section, this chapter).

The foraminifer skeletal packstone of Subunit IIA is generally medium to coarse grained. Skeletal constituents include red algae (corallinaceans, squamariaceans), larger foraminifers (orbitoids), and a few fragments of caprinid rudists; corals, green algae (dasycladaceans), and stromatoporoids are rare. Porosity ranges from 1% to 8% and is mostly moldic. Crusts of bladed, coarsely crystalline calcite line molds and intraparticle pores. The micritic

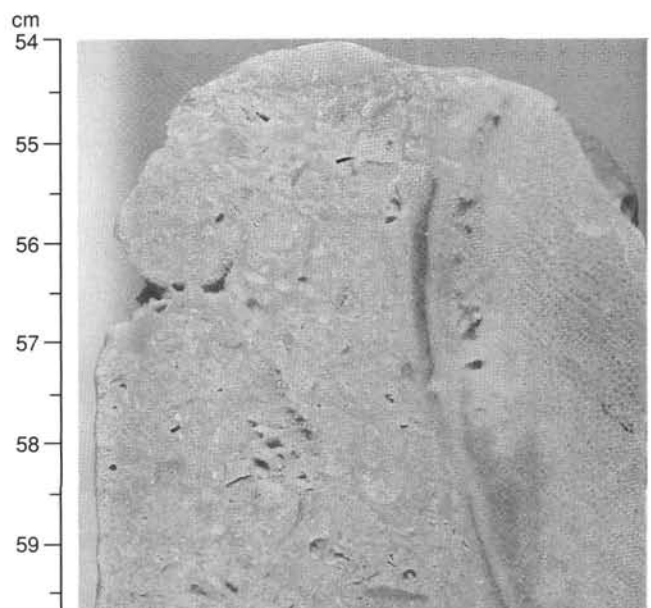


Figure 2. Close-up core photograph of caprinid rudist (Interval 144-877A-1R-2, 54–64 cm).

matrix is about 40%. Solution cavities, millimeter to centimeter sized, are infilled with white to orange-brown micritic internal sediments (e.g., Interval 144-877A-1R-2, 0–37 cm); some of these internal sediments are stained by manganese oxides.

The boundstone includes large fragments of stromatoporoids, corals, caprinid rudists (Fig. 2), and other bivalves that are heavily encrusted (Interval 144-877A-1R-1, 3–24 cm). Typically, they are bound together by red algae (corallinaceans) or, to a lesser extent, by foraminifers and worms. The matrix is a skeletal packstone. Porosity ranges from 1% to 5% and is mostly moldic. Shelter pores are minor and reduced by isopachous crusts of translucent calcite with a probable fibrous habit. Cement in molds is equant, medium-crystalline calcite. Burrowing is pervasive in Interval 144-877A-1R-1, 7–12 cm. Burrows are filled by peloidal skeletal packstone with fragments of radiolitid rudists and red algae; this peloidal skeletal packstone is patchily stained black (by manganese?) and yellow (by phosphate?).

Rudist rudstone includes mainly caprinid and radiolitid rudist fragments, red algae (fragments and crusts of corallinaceans), and larger foraminifers (Interval 144-877A-1R-1, 99–148 cm). Other bivalves, gastropods, stromatoporoids, and green algae (dasycladaceans) are rare in this rudstone. Porosity ranges from 1% to 10% and is mostly moldic with minor additions from intraparticle and interparticle pores. Cements in molds consist of crusts of medium to coarsely crystalline calcite, locally preceded by an isopachous crust of medium crystalline fibrous (?) calcite.

### *Subunit IIB*

Interval: Core 144-877A-2R to Section 144-877A-4R-1, 0 cm
Depths: 9.5–28.4 mbsf
Age: Maastrichtian

The top of Subunit IIB is placed at the top of Core 144-877A-2R and corresponds to a distinct change in sedimentary textures, from predominantly packstone and boundstone in Subunit IIA to skeletal wackestone, packstone, and grainstone in Subunit IIB.

Subunit IIB is comprised of 18.9 m of skeletal wackestone, rudist algal packstone, and grainstone. These lithologies are interbedded in the recovered intervals. The contact between these facies, when recovered, is irregular with local reworking of skeletal wackestone clasts into the packstone and grainstone (e.g., Interval 144-877A-3R-1, 21–27 cm). Sediment color is light gray (10YR 7/2), to very pale brown (10YR 7/3), to white (10YR 8/2) with pinkish (5YR 8/3) patches. In the interval from 9.5 to 28.4 mbsf, the recovery rate averaged 9.3% (see "Operations" section, this chapter). The average calcium carbonate content is 96% (see "Organic Geochemistry" section, this chapter). Geochemical data and X-ray analyses showed that one sample of skeletal wackestone in Subunit IIB (Interval 144-877A-3R-1, 57–64 cm) is locally dolomitic (see "Inorganic Geochemistry" section, this chapter). No dolomite was detected in hand specimens or in thin sections.

The skeletal wackestone of Subunit IIB includes a few molds of thin-shelled bivalves, small gastropods, and rare benthic foraminifers (small miliolids, very rare larger foraminifers). Fragments of rudists (radiolitids and caprinids) are very rare and stained black (pyritized); worm tubes occur sporadically. This wackestone usually displays a color banding of light gray (10YR 7/2) and white (10YR 8/2). There are also irregular, undulating laminations very reminiscent of microbial mats (Interval 144-877A-3R-1, 27–78 cm); this layering is sometimes disrupted, probably as a result of bioturbation. Other evidence of bioturbation is provided by rounded or vertically elongated tubes, a few millimeters in diameter, that are partly filled with white, geopetal micrite (Interval 144-877A-3R-1, 27–78 cm). Edges of cavities are usually sharp and may cut grains of the host rock, suggesting early lithification followed by boring (Interval 144-877A-3R-1, 58–65 cm).

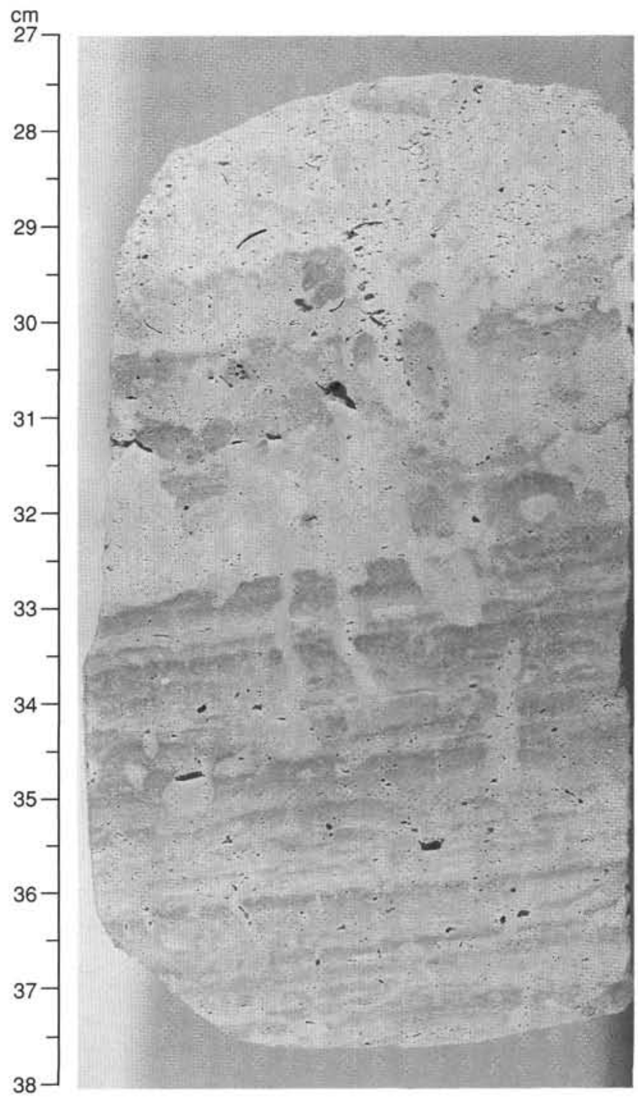

Figure 3. Close-up core photograph of fenestral skeletal wackestone (Interval 144-877A-3R-1, 27–38 cm).

Fenestrae are outstanding features of the wackestone of Subunit IIB (Figs. 3–4). They are usually rounded or may form irregular networks of vertically elongated, tiny canalicules reminiscent of fluid-escape structures. Some fenestrae are aligned horizontally and stacked (Interval 144-877A-3R-1, 27–78 cm), thus emphasizing the laminated aspect of the wackestone ("Laminoid Fenestral Fabric" *sensu* Tebbutt et al., 1965). Porosity averages 10% in the wackestone of Subunit IIB; it is mostly fenestral, moldic (leaching of bivalve and gastropod fragments), and locally vuggy.

The algal rudist packstone and grainstone are poorly sorted, with grain sizes ranging from medium to very coarse sand with minor amounts of gravel. Skeletal components include many caprinid and radiolitid fragments and gastropods; generally, few larger foraminifers (including orbitoids) and red algae are present. Bioclasts are usually angular to subrounded. Thin-shelled bivalves are locally abundant in coarse- to very coarse-grained grainstone (Interval 144-877A-2R-1, 29–73 cm). Porosity aver-

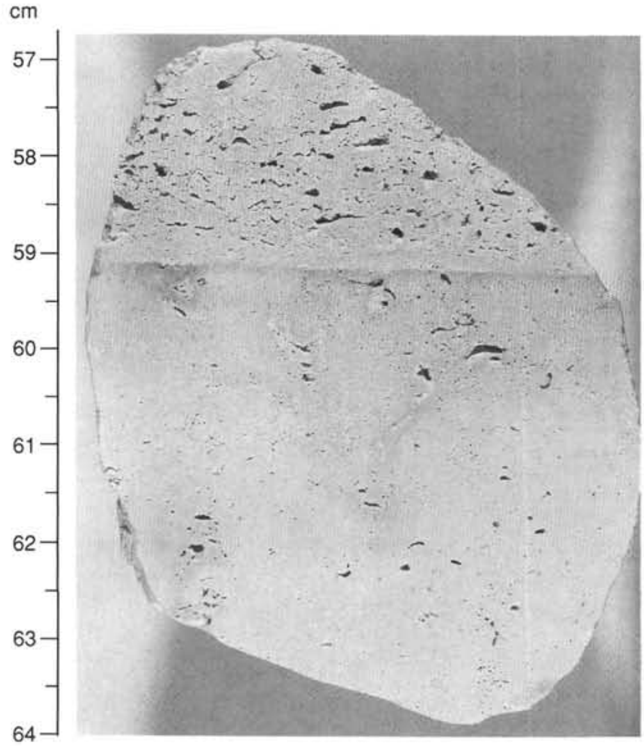


Figure 4. Close-up core photograph of fenestral skeletal wackestone (Interval 144-877A-3R-1, 57–64 cm).

ages 5% and is mostly moldic and intraparticle. Porosity is reduced by calcite cements, including isopachous crusts of coarsely crystalline bladed spars and neomorphic sparry calcite; few of the pores and some millimeter-sized cavities are lined with banded cements. Gastropod molds are partially filled by orange-brown internal sediment. Molds of caprinid rudists may be filled by micrite with small benthic foraminifers, implying a dissolution of the caprinid shells followed by sediment infilling of the moldic pores (Interval 144-877A-3R-1, 0–27 cm).

### *Subunit IIC*

Interval: Core 144-877A-4R to Section 144-877A-12R-1, 0 cm
Depths: 28.4–105.7 mbsf
Age: Maastrichtian

The top of Subunit IIC is placed at the top of Core 144-877A-4R, which corresponds to a change in sedimentary textures from dominantly wackestone and packstone to grainstone, rudstone, floatstone, and boundstone.

Subunit IIC consists of 77.3 m of well-cemented algal-rudist grainstone, rudstone, floatstone, and boundstone with minor foraminifer-rich packstone. These facies alternate in the recovered intervals. The color is very pale brown (10YR 7/3 and 8/3) to white (10YR 8/2). In the interval from 28.4 to 105.7 mbsf, recovery averaged 14.2%, although it was nil between 96 and 105.7 mbsf (see "Operations" section, this chapter). In Subunit IIC, the average calcium carbonate content is 98% (see "Organic Geochemistry" section, this chapter).

Rudists are very abundant throughout Subunit IIC. The assemblage is dominated by loosely packed large caprinids (up to 6 cm in diameter) in Core 144-877A-4R (28.4–38.0 mbsf) and in Core 144-877A-5R (38.0–47.6 mbsf) (Figs. 5–6). A caprinid wall structure was well preserved in Interval 144-877A-5R-3, 103–109 cm (Fig. 7). Geochemical data from this interval show a sharp

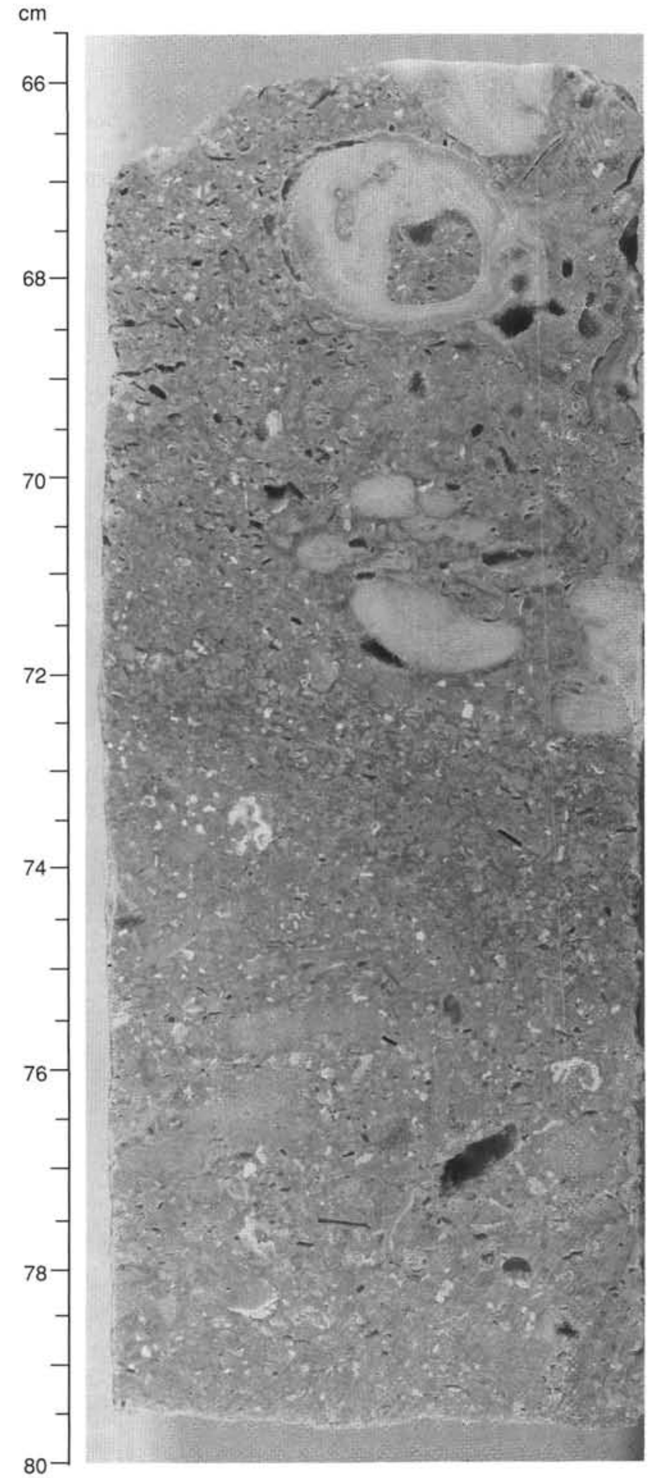


Figure 5. Close-up core photograph of rudist boundstone/rudstone (Interval 144-877A-5R-1, 65–80 cm).

increase in the Sr/Ca ratio, which suggests less diagenetic alteration of the original material (see "Inorganic Geochemistry" section, this chapter). Small radiolitids that are 1 cm in diameter occur locally throughout Subunit IIC. Associated limestones consist of poorly sorted peloid packstone and algal foraminifer peloid

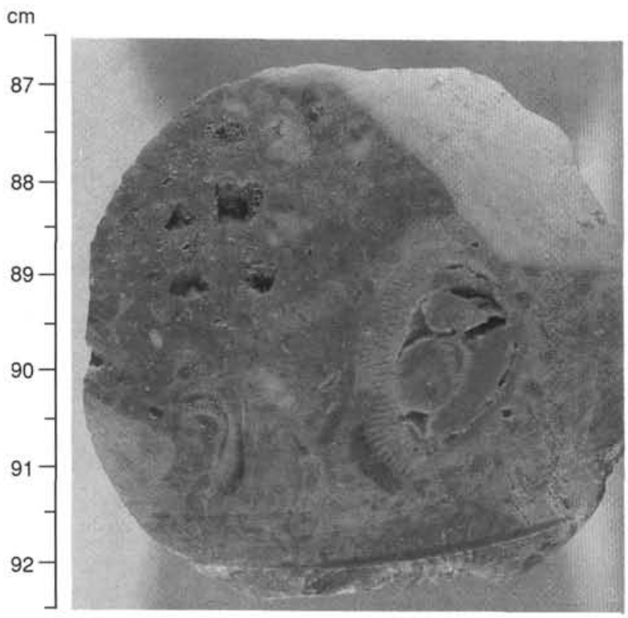


Figure 6. Close-up core photograph of rudist boundstone/rudstone (Interval 144-877A-5R-3, 87–92 cm).

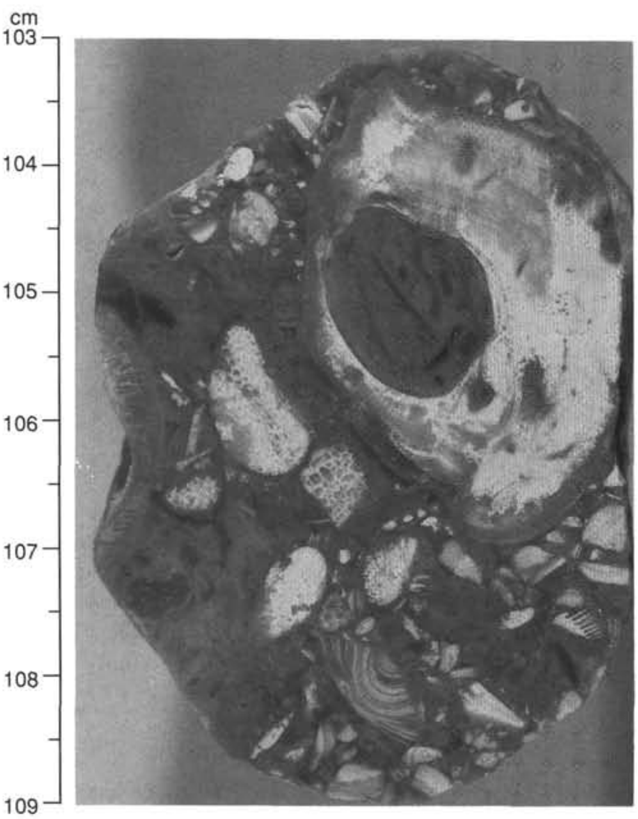


Figure 7. Close-up core photograph of rudist boundstone/rudstone (Interval 144-877A-5R-3, 103–109 cm).

grainstone (generally medium grain sized). In the algal foraminifer peloid grainstone, fragments of red algae (corallinaceans) and larger foraminifers are abundant; few fragments of radiolitid rudists and other bivalves are present. Porosity varies from nil to 5% and is vuggy and moldic. Pores are lined by bladed, medium to coarsely crystalline calcitic crusts, up to several millimeters thick. Intergranular porosity is very low and is mostly filled by translucent to clear intergrown cement crusts.

From Cores 144-877A-6R to -10R (47.6–105.7 mbsf), the assemblage is dominated by small radiolitids that are typically 5–10 mm in diameter and 2–3 cm long. These radiolitids may form clusters of a few individuals, especially in the upper part of the interval from 47.6 to 105.7 mbsf (e.g., Interval 144-877A-6R-1, 90–132 cm) (Fig. 8). Red algae (corallinaceans) may encrust the rudists in life position or, more commonly, encrust tightly packed groupings of various skeletal allochems in the associated sediment (e.g., Interval 144-877A-7R-2, 95–100 cm). The associated sediment consists of skeletal grainstone to packstone with fragments of red algae (corallinaceans and squamariaceans), rudists, and benthic foraminifers (especially miliolids and few orbitoids); gastropods and corals are rare. Porosity averages 3%; it is moldic and intraparticle. Cements in molds consist of crusts either of medium to coarsely crystalline calcite or of equant calcite. In the rudstone facies, porosity may reach 15% and is mostly intraparticle and moldic; cements that fill the pores are crusts of medium crystalline-bladed calcite crusts.

The foraminifer packstone of Subunit IIC is coarse grained and includes abundant larger foraminifers and common fragments of red algae and rudists (caprinids and radiolitids); gastropods and green algae (dasycladaceans) are rare. Most of the grains are micritized and exhibit a micritic envelope (cortoids *sensu* Fluegel, 1982). The porosity ranges from 1% to 10%; it is mostly moldic with minor shelter, boring, and intraparticle porosity. Minor crusts of finely crystalline equant calcite occur in molds.

### *Subunit IID*

Interval: Core 144-877A-12R through Section 144-877A-19R-1, 0 cm
Depths: 105.7–173.2 mbsf
Age: Maastrichtian

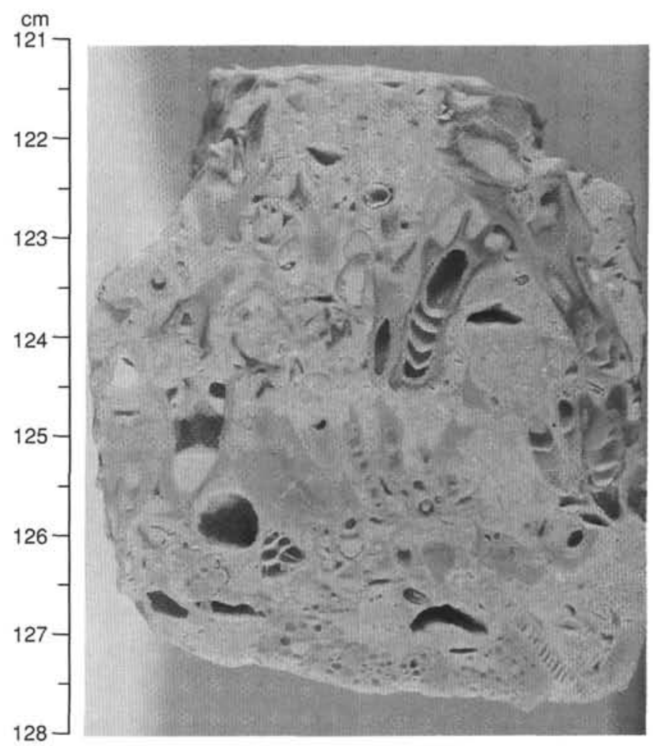


Figure 8. Close-up core photograph of a rudist (radiolitid) cluster (Interval 144-877A-7R-1, 121–128 cm).

The top of Subunit IID (top of Core 144-877A-12R) corresponds to a sharp change in sedimentary texture from predominantly boundstone and rudstone to grainstone. Subunit IID consists of 67.5 m of poorly cemented and friable foraminifer skeletal grainstone with minor amounts of packstone layers. The color is white (10YR 8/2) to light red (2.5YR 6/6). From 105.7 to 173.2 mbsf, the recovery averaged 6.16% (see "Operations" section, this chapter). In Subunit IID, average calcium carbonate content is 98.2% (see "Organic Geochemistry" section, this chapter).

The grainstone of Subunit IID is medium to coarse grained and includes abundant benthic foraminifers (orbitoids, few miliolids), common fragments of red algae, and few fragments of rudists (radiolitids and caprinids). Most grains are recrystallized or chalky. A few lithified domains of packstone occur as the infillings of burrows (Interval 144-877A-15R-1, 0–31 cm). Porosity averages 25% and is mostly solution-enlarged interparticle and moldic.

### *Subunit IIE*

Interval: Core 144-877A-19R through Section 144-877A-20R-1, 20 cm
Depths: 173.2–182.9 mbsf
Age: Maastrichtian

The top of Subunit IIE (top of Core 144-877A-19R) corresponds to changes in color and sedimentary texture from grainstone to packstone and floatstone.

Subunit IIE consists of 9.7 m of poorly sorted foraminifer packstone and floatstone (Interval 144-877A-19R-1, 0–29 cm) (Fig. 9) and well-sorted, fine-grained skeletal foraminifer grainstone (Intervals 144-877A-19R-1, 29–46 cm, and -20R-1, 0–20 cm). The color is brownish yellow (10YR 6/6) to dusky red (2.5YR 3/2), with dark gray (2.5YR N4) to yellow (10YR 7/8) patches. The dusky red color is primarily related to irregular impregnations of iron oxides both in the matrix and in cavities. In Subunit IIE, the average calcium carbonate content is 97.7% at the top of the subunit; it drops to 67.9% at the base of the subunit. At the base of Subunit IIE, the total organic carbon content averages 0.72% (see "Organic Geochemistry" section, this chapter). From 173.2 to 182.9 mbsf, recovery averaged 3% (see "Operations" section, this chapter).

Major components of the packstone and floatstone of Subunit IIE include larger foraminifers (Fig. 9) and fragments of rudists (radiolitids); fragments of red algae (corallinaceans), echinoid spines, and worm tubes are rare. Grains are angular to subangular. Porosity averages 15% and is mostly interparticle to vuggy. Interval 144-877A-19R-1, 0–29 cm, has common lithoclasts of red (10R 5/6) or very dark gray (2.5YR N3) packstone with larger foraminifers.

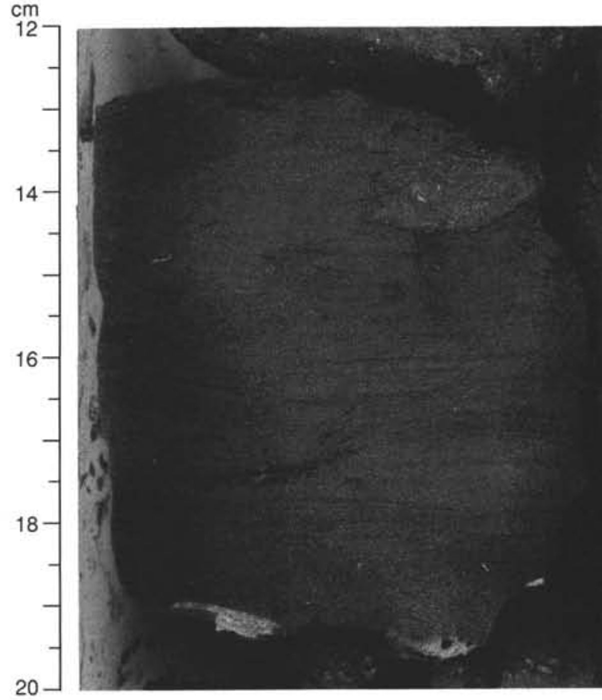

Figure 10. Close-up core photograph of foraminifer grainstone (Interval 144-877A-20R-1, 12–20 cm).

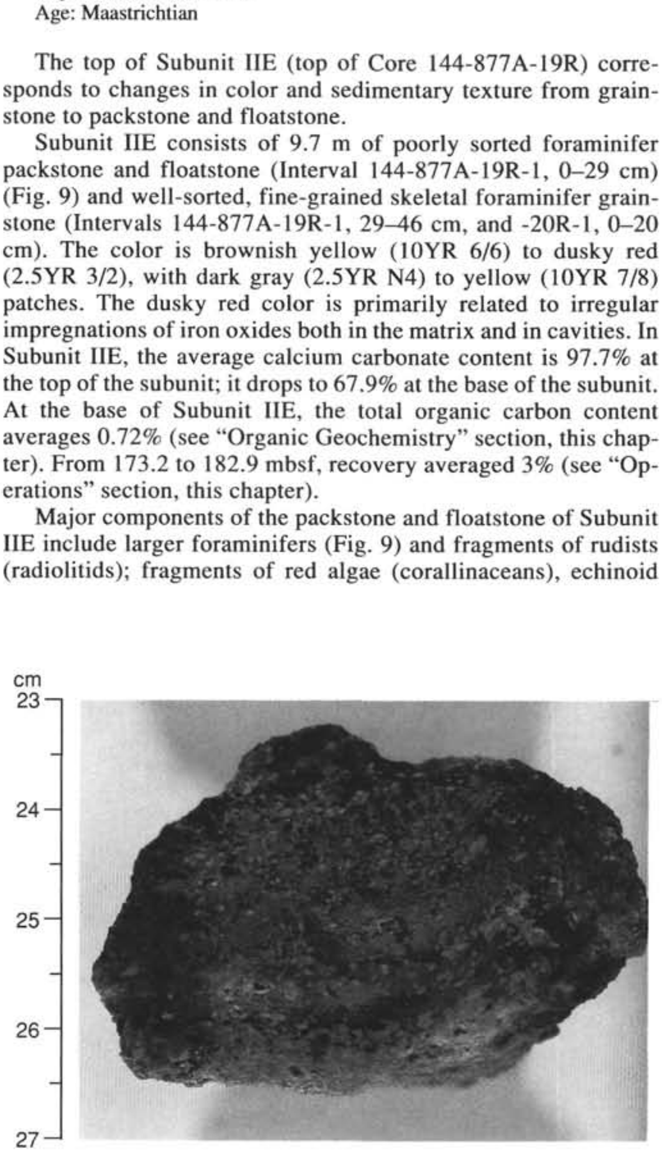

Figure 9. Close-up core photograph of dusky red foraminifer packstone-floatstone (Interval 144-877A-19R-1, 23–27 cm).

The grainstone of Subunit IIE includes abundant fragments of red algae (corallinaceans), recrystallized bioclasts, and larger foraminifers; fragments of radiolitid rudists are rare. Small burrows are reported in Interval 144-877A-20R-1, 0–20 cm (Fig. 10). Pyrite is abundant in Interval 144-877A-20R-1, 0–20 cm, and forms irregular seams; in this interval, sulfur content averages 4.75% (see "Organic Geochemistry" section, this chapter).

## Unit III

Interval: Sections 144-877A-20R-1, 20 cm, through -20R-4, 110 cm
Depths: 182.9–190.2 mbsf
Age: Campanian to indeterminate

The top of Unit III is placed at Section 144-877A-20R-1, 20 cm, at a depth of 182.9 mbsf, in contact with the foraminifer grainstone of Subunit IIE. The base of Unit III is placed at Section 144-877A-20R-4, 110 cm, in contact with the volcanic breccia of Unit IV. Unit III consists of 7.3 m of organic-rich clay, argillaceous limestone, peat, clay, claystone, and claystone breccia. From 182.9 to 190.2 mbsf, the recovery averaged 73.4% (see "Operations" section, this chapter).

The argillaceous limestone of Unit III is fine to medium grained (Interval 144-877A-20R-1, 32–77 cm). Calcium carbonate content averages 44%; the total organic carbon averages 1.48% and the sulfur content averages 8.72% (see "Organic Geochemistry" section, this chapter). This argillaceous limestone includes few thin-shelled mollusc fragments and rare benthic foraminifers. Laminae of black clay are intercalated within these carbonate layers. Interval 144-877A-20R-1, 40–45 cm, contains a nannofossil assemblage of late Campanian age with reworked Cenomanian nannofossils (see "Biostratigraphy" section, this chapter).

The organic-rich clay of Unit III (Intervals 144-877A-20R-1, 20–32 cm, and -20R-1, 77–100 cm) is gray (2.5R N4/0) to black (2.5YR N2.5/0) (Fig. 11). Pyrite is common (5%–10%) and may form microconcretions. The average calcium carbonate content is 0.31% and total organic carbon content averages 20.36%; sulfur content averages 15.2% (see "Organic Geochemistry" section, this chapter).

A black (2.5YR N2.5/0) peat layer is preserved in Interval 144-877A-20R-2, 0–20 cm. The average calcium carbonate content of samples from this interval is 0.28%; total organic carbon content averages 12.45% and the sulfur content averages 23.55% (see "Organic Geochemistry" section, this chapter).

In the Interval 144-877A-20R-2, 46–132 cm, clay is dark brownish gray (10YR 5/3) to very pale brown (10YR 7/4). Contact between colors is gradational. Burrowing is conspicuous. Subvertical and vertical roots, up to 3 cm long, are preserved; the lowest occurrence of roots is in Section 144-877A-20R-2, 120 cm. The average calcium carbonate is 0.42%; total organic carbon content averages 0.65% and the sulfur content averages 10.2% (see "Organic Geochemistry" section, this chapter).

The claystone of Unit III (Sections 144-877A-20R-2, 132 cm, to -20R-3, 90 cm) is laminated; the color is dark brownish and gray within an olive green (5GY 7/4) clayey matrix. Pyrite is common in the matrix (up to 4%) and forms small aggregates. The calcium carbonate content of this claystone averages 0.5% and the total organic carbon averages 0.42%; the sulfur content averages 0.12% (see "Organic Geochemistry" section, this chapter).

The claystone breccia of Unit III (Interval 144-877A-20R-4, 0–110 cm) is made of angular clasts with sizes ranging from 1 mm up to 4 cm. The color of the clasts is very dusky red (2.5R 2/2) to reddish brown (5YR 4/2) in a clayey matrix that is dark greenish gray (5GY 3/4). A clast of basalt is reported in Interval 144-877A-20R-4, 40–44 cm. Horizontal fractures are filled with calcite. The texture of the former igneous breccia is well preserved in Interval 144-877A-20R-4, 100–110 cm.

### Unit IV

Interval: Section 144-877A-20R-4, 110–140 cm
Depths: 187.9–188.2 mbsf
Age: indeterminate

Unit IV consists of gray to dark gray (2.5YR N5/0 to 4/0) volcanic breccia (discussed in the "Igneous Petrology" section, this chapter).

## Comparisons Between Sites 874 and 877 and Preliminary Interpretation of Depositional History

Sites 874 and 877 are located on the inner perimeter ridge of northeastern Wodejebato Guyot (see "Underway and Site Geophysics" section, this chapter) and are separated by about 2.6 km. Site 874 was located on the seaward summit of this ridge, whereas Site 877 was in a slightly more inward position. Furthermore, the topographic relief of the inner ridge seems to be more accentuated in the vicinity of Site 874 than near Site 877 (see "Underway and Site Geophysics" section, this chapter). The top of Hole 877A is 19 m higher (1355 mbsl) than the top of Hole 874B (1374 mbsl).

Although the two sites display a similar succession of sedimentary rocks, some differences in both the lithology and the thickness of units or subunits are noted. Correlations between the two sites are summarized on Figure 12. The thickness of the sedimentary sequence recovered in Hole 874B is 177.7 m; the sedimentary sequence recovered in Hole 877A is 88.2 m.

The depositional history of Site 877 is similar to that of Site 874, although their differences must be stressed if we are to reconstruct the evolution of Wodejebato Guyot during the latest Cretaceous and Early Cenozoic times.

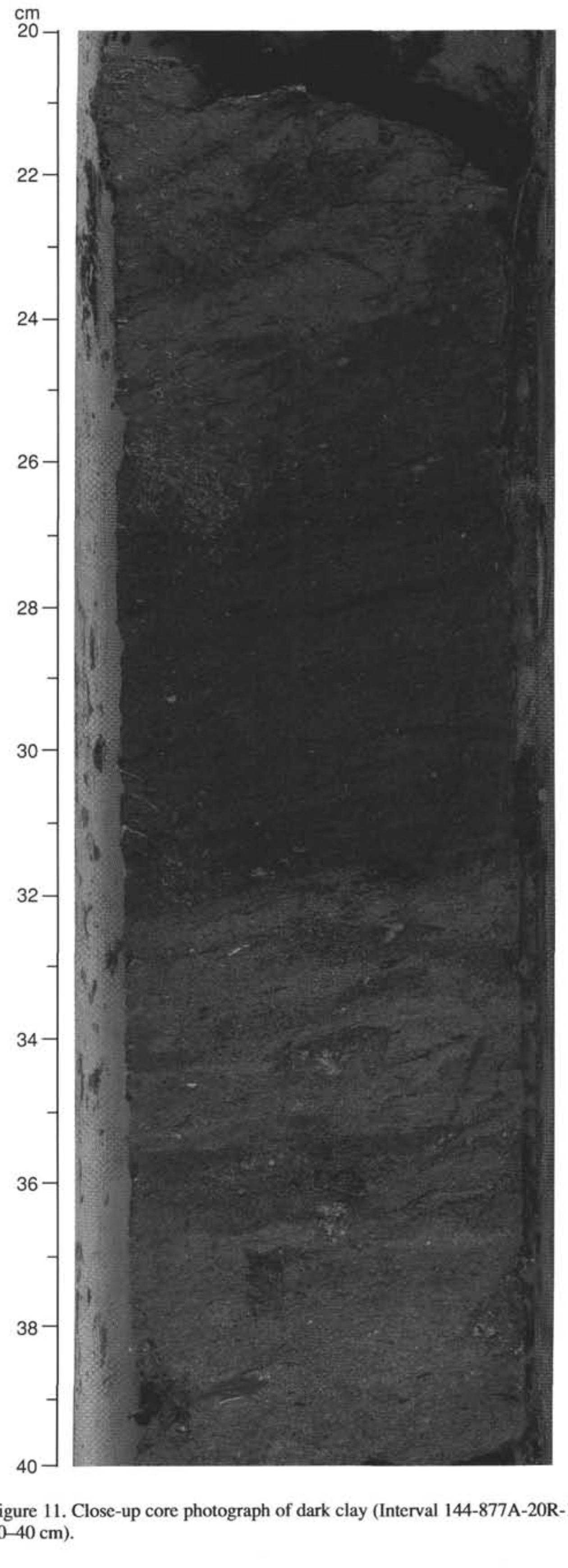


Figure 11. Close-up core photograph of dark clay (Interval 144-877A-20R-1, 20–40 cm).

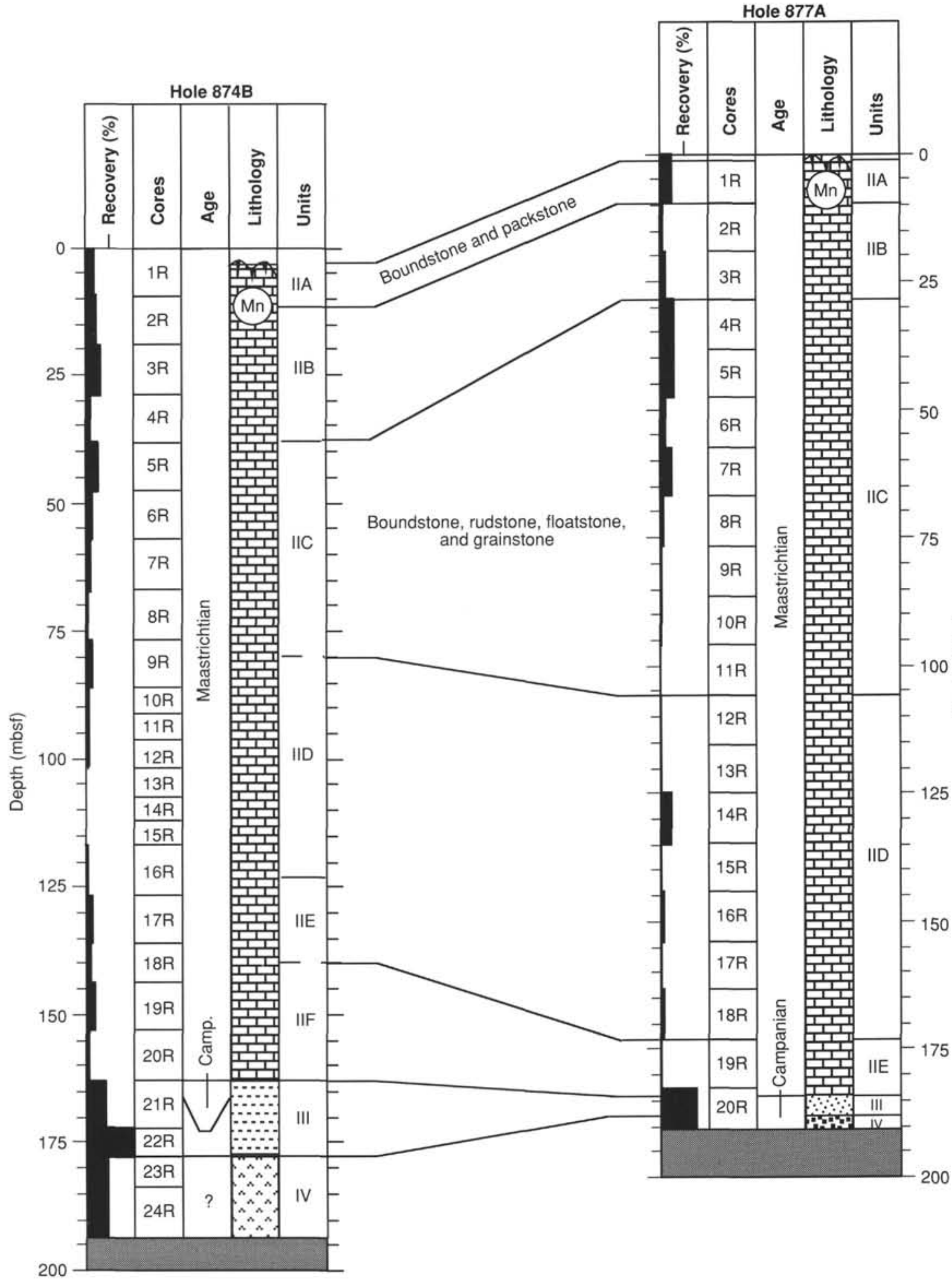


Figure 12. Correlation of the lithostratigraphy between Holes 874B and 877A.

The depositional history of Site 877 began with some form of magmatic eruption and the formation of volcanic breccia encountered at the bottom of the hole (Unit IV).

The clay, claystone, and claystone breccia below Section 144-877A-20R-1 in Unit III are a subaerial weathering profile of the underlying volcanic breccia. The claystone breccia typically has remnant basalt structure and some preservation of basalt clasts. Roots are preserved in Interval 144-877A-1R-2, 46–120 cm. The subaerial weathering profile formed by the clay and claystone is thinner at Site 877 (6.5 m thick; Sections 144-877A-20R-2 through -20R-4; depths, 183.7–190.2 mbsf) than at Site 874 (14.5 m thick; Section 144-874B-21R-1, 41 cm, to Core 144-874B-22R), possibly as a result of the higher basement relief of Site 877.

The top of Unit III documents the flooding of the volcanic island during latest Campanian time. The formation of the peat reported in Interval 144-877A-2R-2, 0–20 cm, may represent the first influences of marine waters. The high sulfur content of this peat is probably related to the bacterial reduction of sulfates provided by marine waters. Preservation of plant debris in this peat suggests the prevalence of low-energy conditions. The organic-rich clay of Unit III (Intervals 144-877A-20R-1, 20–32 cm, and -20R-1, 77–100 cm), which overlies the peat, contains calcareous nannofossils and preserved kerogen-type woody material. The organic-rich clay was deposited in a quiet shallow-marine environment; the high sulfur content suggests the prevalence of reducing conditions. The first carbonate deposits (Interval 144-877A-20R-1, 32–77 cm) are argillaceous limestone with thin-shelled bivalves and rare benthic foraminifers. This indicates a shallow-water environment with low-energy conditions. The preservation of clay and the lack of any reworking at the base of marine deposits are consistent with the prevalence of quiet-water conditions and rapid burial. Organic-rich clay and argillaceous limestone are slightly thicker at Site 877 (0.80 m thick; Interval 144-877A-20R-1, 20–100 cm) than at Site 874 (0.39 m thick; Interval 144-874B-21R-1, 2–41 cm) and does not appear to be an artifact of the percentage of core recovered (see "Operations" section, this chapter, and "Site 874" chapter, this volume).

The platform carbonate sequence is 19.9 m thicker at Site 877 (182.6 m) than at Site 874 (162.7 m). The difference in thickness appears to be related to the differences in thickness of the lower "reef" unit that comprises most of the upper half of the platform carbonate sequence (Hole 877A: Subunit IIC, depths = 28.4–105.7 mbsf, thickness = 77.3 m; Hole 874B: Subunit IIC, depths = 38–80 mbsf, thickness = 42 m). This suggests the elevational difference between the two sites developed as a result of differential reef growth. The underlying subunits of skeletal foraminifer grainstone are slightly thinner at Site 877 (Subunits IID and IIE, depths = 105.7–182.9 mbsf, thickness = 77.2 m) than at Site 874 (Subunits IIE and IIF, depths = 123.5–162.8 mbsf, thickness = 82.4 m).

At Site 877, the platform sequence (Unit II) documents the development and the demise of a Maastrichtian carbonate platform or atoll. Subunit IIE consists of grainstone, packstone, and floatstone deposited in a shallow-marine environment with moderate-to-high energy conditions. Fauna and flora are well diversified and include abundant benthic foraminifers and fragments of red algae and rudists. The occurrence of lithoclasts with larger foraminifers (Interval 144-877A-19R-1, 0–29 cm) indicates a reworking of former platform carbonates. Subunit IIE correlates with Subunit IIF, which was reported at Site 874 (Fig. 12), although no rhodolith was observed in Subunit IIE at Site 877.

Subunit IID consists of poorly cemented, medium- to coarse-grained skeletal grainstone deposited in a shallow-marine environment with moderate-to-high energy conditions; interbedded packstone facies suggest periodic decreases in wave energy. Relative to Subunit IIE, benthic foraminifers (orbitoids and miliolids) in Subunit IID increase in abundance coeval with a decrease in abundance of rudists and red algae. Subunit IID at Site 877 correlates with Subunits IIE and IID at Site 874, although fragments of corals and stromatoporoids are clearly less abundant than in Subunit IID at Site 874. These discrepancies in biotic composition may reflect a zonation related to the different location of the two sites on the inner perimeter ridge of northeastern Wodejebato Guyot.

Relative to Subunit IID, Subunit IIC is characterized by the occurrence of boundstone, rudstone, and floatstone. It corresponds to the first "reef" episode recorded at the edge of the guyot and was deposited in an agitated shallow-marine environment.

Rudists are very abundant throughout Subunit IIC and form the bulk of the organic frameworks. From 47.6 to 105.7 mbsf (Cores 144-877A-6R to -10R), the assemblage is dominated by small erect radiolitids that are usually 5–10 mm in diameter and 2–3 cm long. These radiolitids may form clusters of a few individuals (e.g., Interval 144-877A-6R-1, 90–132 cm); radiolitids in life position are locally encrusted by red algae.

From 28.4 to 47.6 mbsf (Cores 144-877A-4R and -5R), the assemblage is dominated by loosely packed large caprinids (up to 6 cm in diameter); encrusters (e.g., red algae) are very scarce. Large caprinid rudists were typically recumbent and barely attained a gregarious habit (Skelton, 1979); frameworks composed of such forms are normally rather open (Kauffman and Sohl, 1974; Camoin et al., 1988).

Vertical zonation of rudist assemblages may reflect either an evolutionary sequence in reef development or slight changes in environmental conditions. The development of rudist frameworks begins with loose associations and then clusters of small radiolitids from 47.6 to 105.7 mbsf; then, from 38 to 47.6 mbsf, the development of a more open framework with loosely packed assemblages of large caprinids may result from the smothering of the framework by increased sedimentation.

Relative to the first "reef" episode at Site 874 (Subunit IIC), which includes algal-coral boundstone, the development of rudist communities at Site 877 suggests a lateral zonation of the frameworks, probably related to the different location of the two sites on the inner perimeter ridge of northeastern Wodejebato Guyot.

The deposition of Subunit IIB marks a clear change in sedimentation to the deposition of interbedded skeletal fenestral wackestone and rudist algal packstone to grainstone. The contact between these two lithologies is irregular, with local reworking of clasts of wackestone into the packstone and grainstone. These lithologies are consistent with deposition in a shallow lagoon periodically affected by storms, changes in current pattern, or short-term fluctuations of relative sea level; the occurrence of laminar microbial mats and the abundance of fenestrae (e.g., "Laminoid Fenestral Fabric" *sensu* Tebbutt et al., 1965) is consistent with a very shallow depth and possible temporary periods of emergence. Wackestone includes small gastropods and benthic foraminifers, which suggest intermittent restricted conditions. Subunit IIB at Site 877 correlates with Subunit IIB at Site 874, but it is significantly thinner (18.9 m thick at Site 877, and 26.8 m thick at Site 874), probably because of the lower position of Site 877. The coeval occurrence of similar micritic facies at both sites suggests the development of lagoonal sedimentation at the edge of the guyot.

Subunit IIA marks the return to more agitated environments with the deposition of medium- to coarse-grained skeletal packstone, rudist rudstone, and boundstone. The boundstone is made by stromatoporoids, corals, and caprinid rudists that are heavily encrusted by red algae; this structure suggests a "domination" stage of reef evolution (Walker and Alberstadt, 1975). Subunit IIA at Site 877 is very similar to Subunit IIA at Site 874, so that no clear lateral zonation is evidenced in the second "reef" episode at the edge of the guyot.

Pelagic carbonates of late Paleocene to early Eocene age fill cavities in the Maastrichtian platform carbonates (see "Biostratigraphy" section, this chapter); at the top of the platform carbonates, cavities are filled by middle Eocene pelagic sediments (see "Biostratigraphy" section, this chapter).

Diagenetic features in the upper platform carbonates at Site 874 suggest a complex post-depositional history (see "Lithostratigraphy" section, "Site 874" chapter, this volume). The causes of the demise of the Maastrichtian carbonate platform can only be unravelled following detailed shore-based studies.

## BIOSTRATIGRAPHY

### Introduction

A single hole was drilled at Site 877 through approximately 185 m of platform limestones into dark clay and volcanics. Several pieces of manganese crust were recovered from the top of the limestones. Pelagic sediment incorporated into the manganese crust and cavity fillings in the limestones was dated using calcareous nannofossils and planktonic foraminifers. The limestone sequence contains larger foraminifers and rudist bivalves, which are useful for age determinations within the Late Cretaceous. Benthic foraminifer assemblages similar to those observed at Sites 873, 874, 875, and 876 occur. The underlying dark clay was dated by calcareous nannofossils. The biostratigraphy for Hole 877A is given in Figure 13. The preliminary investigations of the different fossil groups are summarized below.

### Calcareous Nannofossils

#### *Manganese Crust*

A thin section of Sample 144-877A-1R-1, 1–4 cm, is comprised of sedimentary rock surrounded by a manganese crust from the top of the cored sequence. Most of the sediment consists of Cretaceous platform carbonate debris similar to the underlying limestone and heavily phosphatized material of uncertain age. Several large voids, lined with a bladed cement crust, have been subsequently filled with pelagic limestone containing well-preserved nannofossil assemblages. Species present include *Discoaster kuepperi, Discoaster lodoensis, Discoaster barbadiensis, Reticulofenestra dictyoda, Sphenolithus editus,* and *Campylosphaera dela,* indicating Zone CP11 of late early Eocene age.

#### *Cavity Filling in Limestones*

Infillings of small, manganese-lined pockets in the top of first piece recovered in Core 144-877A-2R (Sample 144-877A-2R-1, 0–1 cm), consist of white nannofossil ooze with abundant, very well-preserved nannofossils including *Discoaster multiradiatus, Camplyosphaera eodela, Fasciculithus tympaniformis* (s.s.), *Neococcolithes protenus,* and *Placozygus sigmoides.* This assemblage identifies Subzone CP8b of latest Paleocene age. The assemblage sampled from these manganese-lined pockets is unusual in that it appears to totally lack any *Sphenolithus primus.* This lack of sphenoliths may indicate cooler surface-water conditions (Perch-Nielsen, 1985). A similar assemblage, albeit with *S. primus,* occurs as very pale brown nannofossil ooze fillings of obvious voids within the cemented platform carbonates of Core 144-877A-2R (e.g., Samples 144-877A-2R-1, 7–11 cm, and -2R-1, 14–19 cm). Preservation in the very pale brown ooze is also excellent, although the nannofossil assemblages are diluted with micrite.

#### *Dark Clay*

A sequence of dark, carbonaceous clay and argillaceous limestone in Core 144-877A-20R immediately underlies the platform carbonate sequence. Samples from several intervals within Section 144-877A-20R-1 contain sparse calcareous nannofossils. The richest of these assemblages (from Interval 144-877A-20R-1, 42–45 cm) contain *Quadrum trifidum, Quadrum sissinghii, Arkhangelskiella specillata,* and *Reinhardtites anthophorus,* indicating Zone CC22 of late Campanian age. Reworked taxa of Cenomanian age include *Corollithion kennedyi, Parhabdolithus asper,* and *Axopodorhabdus albianus.* Preservation is good and diversity high. Several species are represented by specimens smaller than their usual size, and a number of new taxa were observed.

### Planktonic Foraminifers

#### *Manganese Crust*

The surface of the platform limestone is marked by a thin manganese crust that was recovered in Core 144-877A-1R-1, 0–4 cm, just below the surface. Planktonic foraminifers were observed only in a small patch, and these are poorly preserved. The identification of *Turborotalia pomeroli* associated with some subbotinids indicates an age not older than middle Eocene Zone P12. The manganese phosphatic limestone from Hole 877A seems, at first sight, to differ from those recovered at Sites 873 through 876, although this may be an artifact of drilling and/or lack of recovery. At Site 877, the manganese crust is somewhat reduced in thickness. In comparison with the other sites, the recovered material seems confined to the inner, thus older, part of the crust.

#### *Cavity Filling in Limestones*

An infilled cavity in Sample 144-877A-1R-1, 8–10 cm, contains few to common, poorly preserved planktonic foraminifers from Subzone P3b/Zone P4 of late Paleocene age. Species identified include *Morozovella conicotruncata, M. aequa, "Subbotina" pseudobulloides,* and *Acarinina soldadoensis.* A few fish teeth are also present. Also occurring in Sample 144-877A-1R-1, 8–10 cm, are a few very poorly preserved planktonic foraminifers of middle Maastrichtian age. Species identified include *Globotruncana ventricosa, Pseudotextularia elegans,* and a possible *Gansserina gansseri.* These planktonic foraminifers are associated with platform debris.

In Sample 144-877A-3R-1, 9–11 cm, a cavity infilling contains common to frequent planktonic foraminifers from Subzone P6b of early Eocene age. Species identified include *Morozovella gracilis, M. subbotinae, M. aequa, M. wilcoxensis, Acarinina intermedia, A. soldadoensis, A. angulosa, Pseudohastigerina wilcoxensis,* and *Planorotalites chapmani.* Also present are rare to few planktonic foraminifers of Subzone P3b/Zone P4 (late Paleocene), including *Planorotalites compressus, Morozovella aequa, Subbotina triloculinoides, "S." pseudobulloides,* and *Guembelitria* sp.

#### *Platform Limestones*

Planktonic foraminifers are rare in the platform limestone sequence of Hole 877A. Those that occur are consistent with the Late Cretaceous age inferred from the other sites on Wodejebato Guyot. In Sample 144-877A-7R-2, 109–120 cm, the species *Archaeoglobigerina cretacea, Rugoglobigerina rugosa,* and *Globotruncana arca* were identified. In Sample 144-877A-18R-1, 25–28 cm, the species *Globigerinelloides ultramicrus, Archaeoglobigerina* sp., *Globotruncana* sp., and *Heterohelix globulosa* are present. A possible *Rugoglobigerina* was observed in Sample 144-877A-19R-1, 27–30 cm.

### Larger Benthic Foraminifers

The 182.9-m-thick sequence of platform limestone (Lithologic Unit II) recovered in Hole 877A (Core 144-877A-1R to Section 144-877A-20R-1, 20 cm) yielded abundant larger benthic foraminifers associated with abundant rudist bivalves, especially in the upper half of the unit; also found are coralline algae, echinoid fragments, and common corals. The distribution of the microfauna and associated forms from the platform carbonates in Hole 877A was based on observations of the core surface, thin sections, and specimens isolated from the saw cuttings from each section of the split core.

The distribution of larger foraminifers in Hole 877A varies with facies distribution throughout the platform sequence. As far as can be inferred from the limited number of thin-section samples examined at present, assemblages tend to be fairly continuous, with the exception of the uppermost portion, in which the facies is very poor in foraminifers and even algae (Cores 144-877A-2R and -3R). The sequence of benthic foraminifer assemblages (labeled I, II, III and IV) parallels those observed in Hole 874B. These assemblages have been described at Sites 873 and 874 (see "Biostratigraphy" sections, "Site 873" and "Site 874" chapters, this volume). The boundaries of the assemblages are tentatively indicated on Figure 13, pending more detailed investigations.

### Rudists

Rudists, both caprinids and radiolitids, occur throughout the Maastrichtian platform limestone sequence of Hole 877A. They were briefly examined during the cruise and will require more study.

Rudists are especially abundant in Lithologic Subunits IIA (0.03–9.5 mbsf) and IIC (28.4–105.7 mbsf), in which they form loosely packed settlements or, more rarely, clusters of a few individuals (see "Lithostratigraphy" section, this chapter). In the other lithologic subunits, they are generally fragmented or poorly preserved.

In the interval from 0.03 to 47.6 mbsf (Cores 144-877A-1R to -6R), the assemblage is dominated by loosely packed settlements of large caprinids. Small radiolitids that are approximately 1 cm in diameter occur locally. Some large caprinids, up to 6 cm in diameter, exhibit numerous small polygonal and rounded canals, which are mostly tabulate, throughout their shell (see Figs. 2 and 7; "Lithostratigraphy" section, this chapter); an outer set of oval canals is locally present. These forms may belong to the *Antillocaprina–Titanosarcolites* group. However, the large tubular canals that characterize the anteroventral side of the shell of *Titanosarcolites* were not observed in the available samples. Some other caprinid specimens display narrow elongate canals separated by bifurcate radial plates (see Fig. 6; "Lithostratigraphy" section, this chapter), a structure very reminiscent of caprinids from the *Plagioptychus* group. Few specimens exhibit a free valve with two rows of rounded or polygonal pallial canals and one of two outer rows of pyriform canals; these may correspond to *Mitrocaprina*.

In the interval from 47.6 to 105.7 mbsf (Cores 144-877A-7R to -12R), the assemblage is dominated by small radiolitids (see Fig. 8; "Lithostratigraphy" section, this chapter), which are typically 5–10 mm in diameter and 2–3 cm long, and which locally form clusters of a few individuals (e.g., Interval 144-877A-6R-1, 90–132 cm).

The caprinids from the *Antillocaprina–Titanosarcolites* group have been previously reported only from the Maastrichtian strata of the Caribbean (Puerto Rico, Cuba, Jamaica; Kauffman and Sohl, 1974). The genera *Plagioptychus* and *Mitrocaprina* are cosmopolitan, having been reported from the Cenomanian to Maastrichtian of many Tethyan areas.

### Siliceous Microfossils

Seven samples from Hole 877A were processed on board for quantitative analysis of the HCl-insoluble residue.

#### *Platform Carbonates*

Small amounts of marine siliceous microfossils are present throughout the Campanian-Maastrichtian limestone sequence, with the exception of Sample 144-877A-19R-CC, which is barren.

In the white, fossil-rich limestones of the upper part of the sequence (Samples 144-877A-1R-CC to -14R-CC), siliceous sponge spicules (monaxons) and fragments of radiolarians are very rare, with measured abundances of between 0.03 and 0.34 specimens per gram of sediment. In addition, single marine planktonic diatoms occur in these well-cemented fossiliferous limestones. In Cores 144-877A-5R and -8R, freshwater diatoms (*Aulacosira granulata*) are present. Most probably these findings are the result of contamination. Whether this is also the case for the sponge spicules and the radiolarians, cannot be decided.

In the limestones below Sample 144-877A-15R-CC, only sponge spicules are present. In this lower portion of Lithologic Unit II, the sponge spicules are relatively abundant, up to 1.7 sponge spicules per gram of sediment.

#### *Claystone and Peat*

One sample from Lithologic Unit III was analyzed (Sample 144-877A-20R-1, 100 cm). This organic-rich, dark clay contains abundant plant remains and pyrite, as well as a small radiolarian fragment and a few monaxon sponge spicules. Thus, as at Site 873, the upper part of the claystone, which underlies the platform carbonates, clearly documents a marine influence, either by occasional flooding or by clay deposition in a marine environment.

### Palynology

Two samples from the dark clay (Lithologic Unit III) in Hole 877A were processed for palynology. For each sample, effective concentration of the >20 μm organic fraction was obtained by treating the sample with 20% HCl, sieving it at 20 μm, and then swirling it in a watch glass. Sample 144-877A-20R-2, 96–98 cm, is a light gray, silty clay from the lower part of Lithologic Unit III that contains traces of rootlets. The residue was found to consist entirely of moderately preserved woody tissues and cuticle, with some pyrite impregnation. Sample 144-877A-20R-1, 30–32 cm, is a black, silty sediment from the dark, organic-rich upper part of the unit. The residue is rich in pyrite and dominated by woody tissues; however, sporadic palynomorphs, including a multicellate fungal spore, several fern spores assignable to *Leiotriletes*, a probable foraminifer lining, and several thin-walled, crumpled acritarchs provisionally referred to *Leiosphaera* that might be of algal affinity were all visible.

### Summary

The sequence recovered at Site 877 is comparable with that recorded at Site 874, which was also drilled on the "inner perimeter ridge" of Wodejebato Guyot. At Site 877, the dark clay and claystone above the volcanics yielded palynomorphs and a nannofossil assemblage similar to that seen in the dark clays of Hole 874B. However, the nannofossils that occur are more usefully age-diagnostic than those that occur in Hole 874B; as such, they indicate a late Campanian age. Furthermore, the presence of rare reworked Cenomanian nannofossils in the clay at this site are the only indication so far recorded of an earlier, pre-Campanian history to the guyot.

The platform limestones also contain similar faunas and floras to those described from Hole 874B, and in the same sequence, indicating a similar environmental history (see "Biostratigraphy" section, "Site 874" chapter, this volume). Furthermore, the nannofossils and planktonic foraminifers from void fillings in the limestones and incorporated in the manganese crust also indicate a similar history for the two sites following drowning of the carbonate platform in the Maastrichtian.

## PALEOMAGNETISM

The susceptibility of limestone cores from Hole 877A was not measured because of the low average recovery (13%). Measurements of the initial magnetic susceptibility were conducted at 5-cm intervals for claystone and basalt in Core 144-877A-20R (Fig. 14). Susceptibility varies by a factor of 1000 in this core, and these variations closely reflect changes in lithology (see

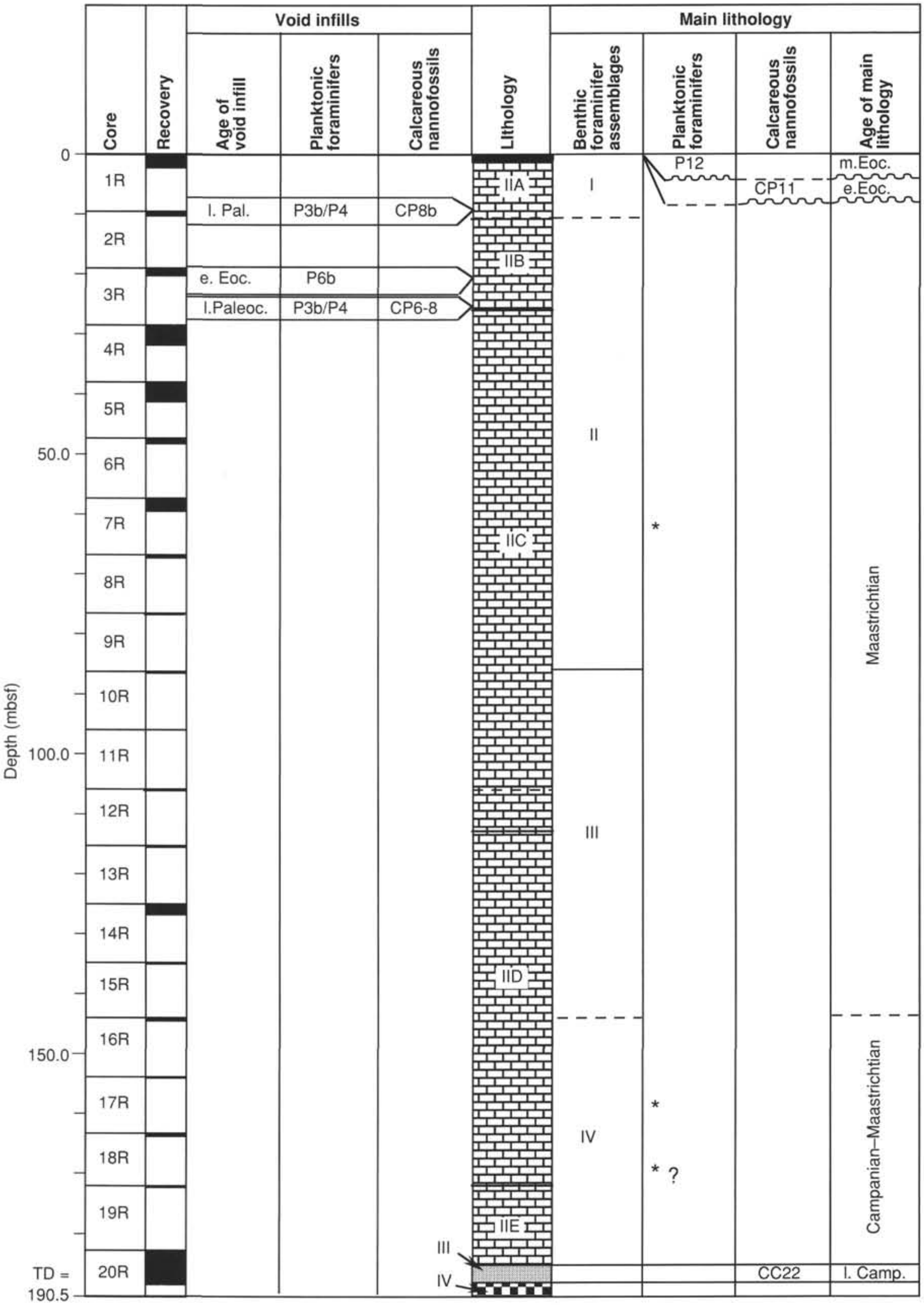


Figure 13. Biostratigraphy of Hole 876A. Asterisks indicate the occurrence of planktonic foraminifers. TD = total depth.

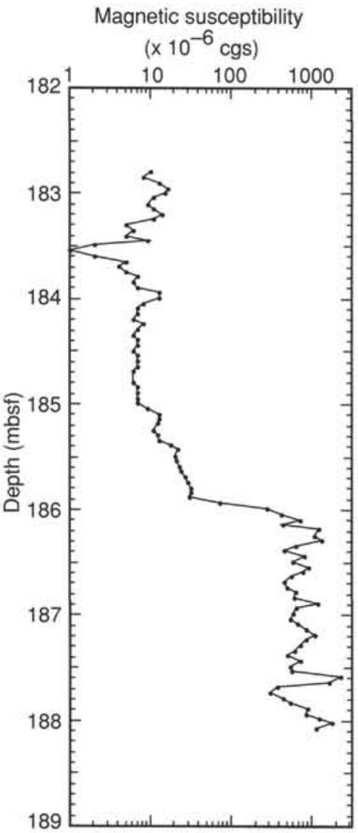


Figure 14. Magnetic susceptibility variations for claystone from Hole 877A.

"Lithostratigraphy" section, this chapter). For example, the lower susceptibility near 183.5 mbsf corresponds to the contact between the overlying argillaceous limestones and the underlying black clays. The latter unit, including a 20-cm-thick peat layer near 184 mbsf, is characterized by low values of susceptibility, presumably a result of the reducing conditions. The downhole increase in susceptibility over the interval from 185 to 186 mbsf coincides with a gray/green clay. The marked increase in susceptibility at 186 mbsf marks the contact with a reddish claystone. The susceptibility of this reddish claystone (ca. $10^{-3}$ cgs) is indistinguishable from that of the underlying basalt/volcaniclastic breccia (>187.9 mbsf).

Natural remanent magnetization (NRM) and the remanence after 15-mT alternating-field (AF) demagnetization were measured for several long continuous pieces of the limestone in Cores 144-877A-1R through -7R. These larger volume samples were measured using the pass-through cryogenic magnetometer in discrete sample mode as for limestone samples from Site 874. We were unable to determine a magnetostratigraphy; however, the higher sensitivity of shore-based magnetometers should be sufficient to determine the characteristic magnetization of the limestone samples.

The archive halves of Core 144-877A-20R (182.9–190.0 mbsf) were also measured after AF demagnetization using the pass-through cryogenic magnetometer. Accurate determination of the remanent magnetization was precluded by repeated flux jumps.

Two discrete samples of basalt were measured with the pass-through cryogenic magnetometer after AF demagnetization (Table 3). The demagnetization behavior of the two samples is shown in Figures 15 and 16. The inclination of the characteristic remanence magnetization (ChRM) at Hole 877A is positive and is similar to that of samples from elsewhere on the guyot (Sites 872–876). The simplest explanation is that these positive inclinations represent a reversed polarity magnetization acquired in the Southern Hemisphere. The results from Site 877 alone suggest a

**Table 3. Results of demagnetization of basalts from Hole 877A.**

| Core, section, interval (cm) | Lithology | Inclination (degrees) |
|---|---|---|
| 144-877A- | | |
| 20R-4, 115–117 | Basalt | +8.9 |
| 20R-5, 14–16 | Basalt | +14.2 |

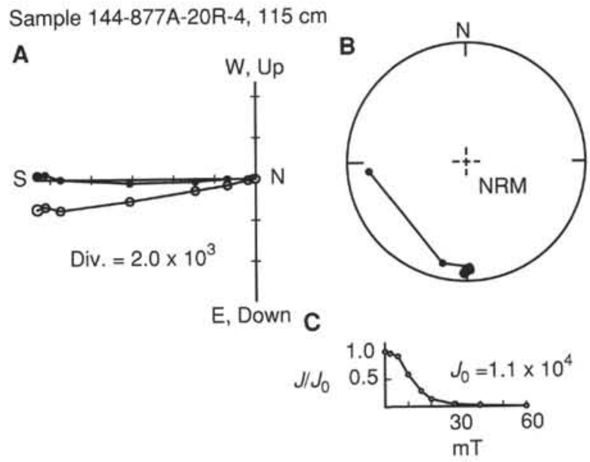


Figure 15. Alternating-field (AF) demagnetization results for basalt Sample 144-877A-20R-5, 115 cm. Demagnetization fields are 0, 2.5, 5, 10, 15, 20, 29, 40, and 60 mT. **A.** Orthogonal vector plot of the progressive AF demagnetization. Closed circles represent horizontal components of the magnetization, and open circles represent vertical components. **B.** Stereonet plot of vector endpoints after progressive demagnetization. **C.** Variation of intensity after progressive AF demagnetization.

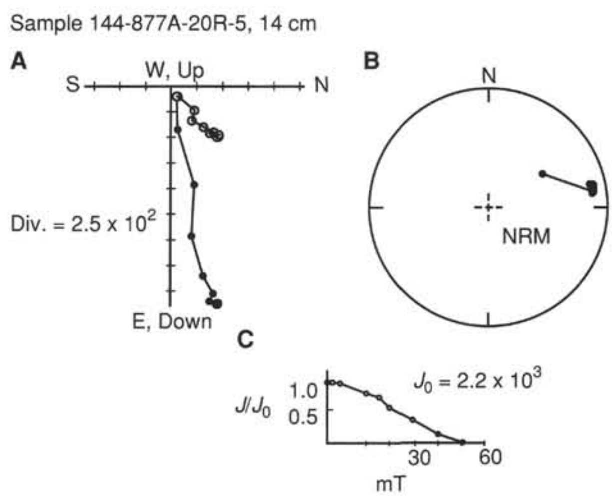


Figure 16. Alternating-field (AF) demagnetization results for basalt Sample 144-877A-20R-5, 14 cm. Demagnetization fields are 0, 2.5, 5, 10, 15, 20, 29, 40, and 60 mT. Other plot conventions are identical to Figure 15.

Table 4. Surface seawater and interstitial water geochemical data, Hole 877A.

| Core, section, section (cm) | Depth (mbsf) | pH | Alkalinity (mM) | Salinity (g/kg) | $Cl^-$ (mM) | $Mg^{2+}$ (mM) | $Ca^{2+}$ (mM) | $SO_4^{2-}$ (mM) | $NH_4^+$ (µm) | $SiO_2$ (µm) | $K^+$ (mM) | Rb (µm) | $Sr^{2+}$ (µm) | $Na^+$ (mM) | F (µm) | Li (µm) |
|---|---|---|---|---|---|---|---|---|---|---|---|---|---|---|---|---|
| Surface seawater | 0 | — | — | 35.0 | 560 | 64.24 | 10.61 | 28.8 | 178 | 0 | 10.00 | 1.40 | 91 | 477 | 73 | 26 |
| 144-877A- | | | | | | | | | | | | | | | | |
| 20R-3, 140–150 | 186.67 | 7.62 | 2.81 | 35.0 | 559 | 62.96 | 11.36 | 29.4 | 35 | 146 | 9.24 | 1.57 | 100 | 479 | 96 | 36 |

Table 5. Lithologic geochemical data, Hole 877A.

| Core, section, interval (cm) | Depth (mbsf) | Mg/Ca ($\cdot 10^2$) | Sr/Ca ($\cdot 10^3$) | F/Ca ($\cdot 10^3$) | $SiO_2$/Ca ($\cdot 10^3$) | $PO_4$/Ca ($\cdot 10^3$) | Fe/Ca ($\cdot 10^3$) | Mn/Ca ($\cdot 10^4$) |
|---|---|---|---|---|---|---|---|---|
| 144-877A- | | | | | | | | |
| 1R-1, 54–57 | 0.54 | 1.46 | 0.40 | 0.16 | 1.78 | 0.64 | 0.11 | 0.22 |
| 1R-2, 73–75 | 1.21 | 1.70 | 0.36 | 0.23 | 1.88 | 0.82 | 0.17 | 0 |
| 2R-1, 6–13 | 9.56 | 1.99 | 0.46 | 3.42 | 17.56 | 10.06 | 1.90 | 8.51 |
| 3R-1, 57–64 | 19.57 | 18.67 | 0.44 | 1.52 | 2.54 | 5.35 | 0.29 | 0.24 |
| 4R-1, 7–15 | 28.47 | 2.05 | 0.87 | 0.51 | 0.94 | 1.80 | 0.14 | 0.19 |
| 4R-2, 37–42 | 30.28 | 2.12 | 0.31 | 0.03 | 9.93 | 0.47 | 0.73 | 0.20 |
| 5R-1, 56–60 | 38.56 | 2.10 | 0.45 | 0.27 | 0.00 | 0.40 | 0.24 | 0.26 |
| 5R-3, 51–55 | 41.50 | 2.06 | 0.62 | 0.36 | 0.93 | 0.49 | 0.13 | 0.29 |
| 5R-3i, 73–78 | 41.72 | 3.89 | 1.22 | 0.66 | 0.96 | 0.61 | 0.18 | 0.33 |
| 5R-3ii, 73–78 | 41.72 | 5.09 | 1.40 | 0.93 | 0.13 | 0.76 | 0.15 | 0.27 |
| 6R-1, 62–66 | 48.22 | 1.73 | 0.37 | 0.34 | 1.85 | 0.56 | 0.32 | 0.28 |
| 7R-1, 121–128 | 58.51 | 1.40 | 0.76 | 0.86 | 0.97 | 0.45 | 0.21 | 0.57 |
| 8R-1, 116–120 | 68.16 | 1.62 | 0.34 | 0.28 | 0.94 | 0.80 | 0.12 | 0.28 |
| 20R-5, 27–28 | 188.45 | 5.59 | 0.24 | 3.32 | 143.00 | 0.90 | 27.56 | 208.86 |

paleolatitude of about 6°S; the combined data from all sites on Wodejebato Guyot yield a paleolatitude near 10°S.

# INORGANIC GEOCHEMISTRY

## Interstitial Waters

Interstitial waters were taken from one core sample in Hole 877A and analyzed according to the methods outlined in the "Explanatory Notes" chapter (this volume). This sample came from clays. No interstitial water samples were taken from the overlying or underlying units. Shipboard interstitial water data from Site 877 are presented in Table 4.

### *Salinity and Chlorinity*

Salinity and chlorinity of the pore water sample from Hole 877A are indicative of normal seawater (Table 4).

### *Alkalinity, pH, Calcium, Magnesium, Sodium, Potassium, Rubidium, Strontium, and Lithium*

The pH and alkalinity values and measured sodium and rubidium concentrations are in the range of normal seawater. Calcium, magnesium, potassium, strontium, and lithium concentrations are consistent with limited chemical exchange between pore waters and the clays. Pore waters are moderately enriched in calcium, strontium, and lithium with respect to seawater, whereas they are depleted in magnesium and potassium (Table 4).

### *Silica*

Silica concentrations in the interstitial water sample from Hole 877A are in the range of seawater (Table 4).

### *Sulfate and Ammonium*

Sulfate and ammonium concentrations in the interstitial water sample from Hole 877A are indicative of normal seawater (Table 4).

### *Fluoride*

Fluoride concentrations in the interstitial water sample from Hole 877A are enriched with respect to normal seawater (Table 4).

## Lithologic Data

Fourteen rock samples were taken from the split core from Hole 877 and analyzed according to the methods outlined in the "Explanatory Notes" chapter (this volume). Thirteen of these samples came from limestones and one, Sample 144-877A-20R-5, 27–28 cm, came from a vein in the underlying volcanic breccia. Data are expressed as molar ratios to calcium for both minor and trace elements: ($Mg/Ca \cdot 10^2$), ($Sr/Ca \cdot 10^3$), ($F/Ca \cdot 10^3$), ($PO_4/Ca \cdot 10^3$), ($SiO_2/Ca \cdot 10^3$), ($Fe/Ca \cdot 10^3$), and ($Mn/Ca \cdot 10^4$). Shipboard rock-sample data from Site 877 are presented in Table 5.

### *Magnesium, Strontium, Fluoride, and Phosphate*

Magnesium/calcium and strontium/calcium ratios in rock samples from Hole 877A range from 1.40 to 18.67 and 0.24 to 1.40, respectively. Magnesium/calcium ratios in the range of 1.40 to ~2.20 and strontium/calcium ratios in the range of 0.24 to ~0.60 are consistent with the alteration of metastable aragonite and high-magnesian calcite to more stable low-magnesian calcite (<3 mM) (Fig. 17). The magnesium content of Sample 144-877A-3R-1, 57–64 cm (18.67 mM) suggests the presence of dolomite. An X-ray diffraction (XRD) analysis on Sample 144-877A-3R-1, 57–64 cm, confirmed the presence of dolomite (Fig. 18). This sample was located in white wackestone (see "Lithostratigraphy" section, this chapter).

Fluoride/calcium and phosphate/calcium ratios in rock samples from Hole 877A range from 0.16 to 3.42 and from 0.40 to 10.06, respectively; these values are indicative of the presence of some form of fluorapatite (Fig. 17). Sample 144-877A-2R-1, 6–13 cm, is remarkable, both because it has a high fluorapatite content (10 µM phosphate), and because it is a manganiferous limestone cavity-fill containing pelagic material identified as late Paleocene in age (see "Lithostratigraphy" and "Biostratigraphy" sections, this chapter).

### *Silica, Iron, and Manganese*

Silica/calcium ratios in rock samples from Hole 877A range from 0.13 to 143.00 and are indicative of metastable silica, that is the silica that dissolves in 10% HCl (Fig. 17). High silica contents are associated with the sample from the basalt as well as the sample containing the pelagic material (Samples 144-877A-20R-5, 27–28 cm, and -2R-1, 6–13 cm). Iron/calcium and manganese/calcium ratios range from 0.11 to 27.56 and from 0 to 208.86, respectively (Fig. 17).

## Summary

Site 877 data are consistent with (1) chemical exchanges between clays and their interstitial waters, (2) alteration of metastable aragonite and high-magnesian calcite to more stable low

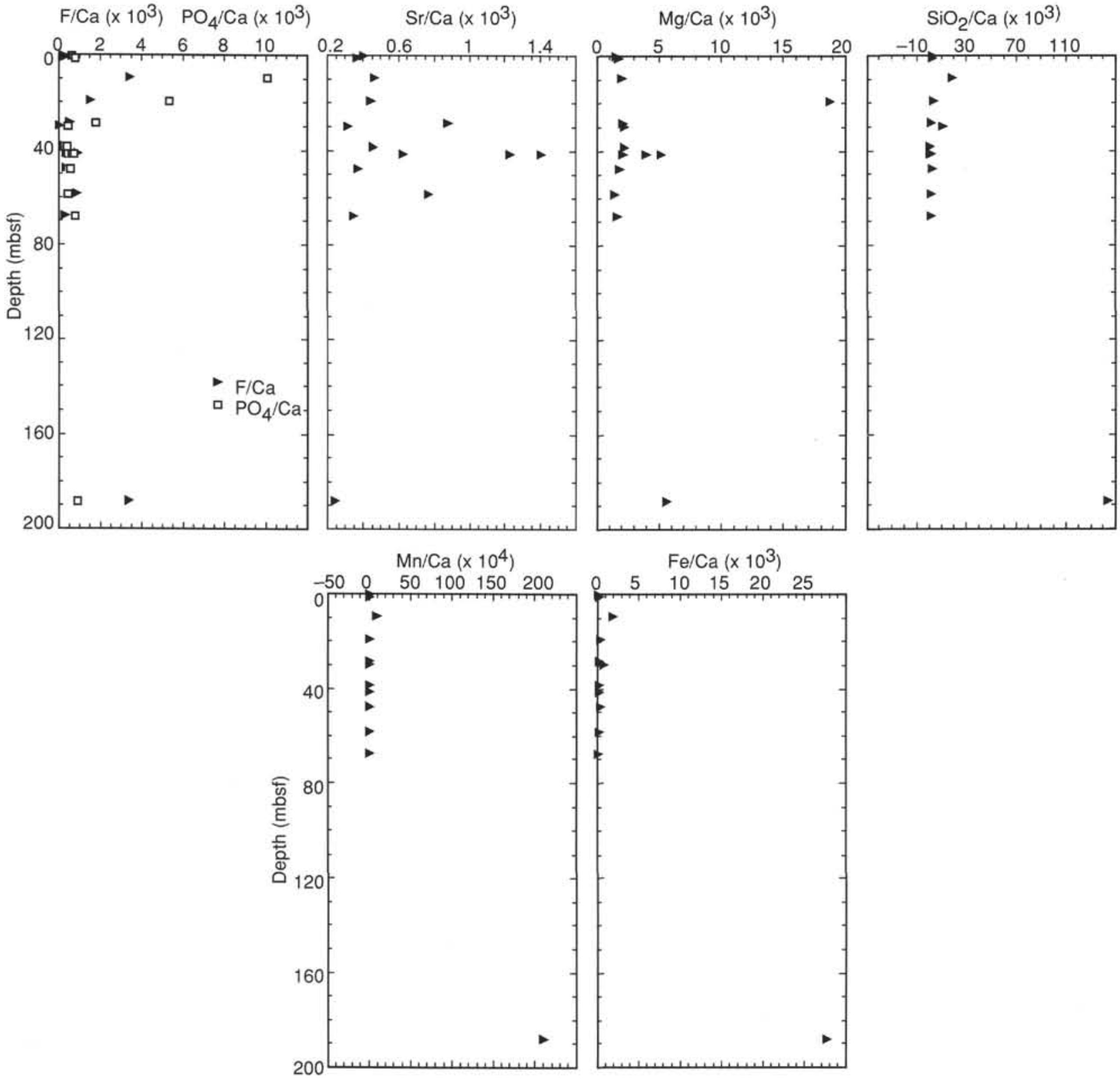


Figure 17. Elemental abundances of rock samples vs. depth, Hole 877A. Abundances are expressed as a molar ratio with respect to calcium.

magnesian calcite in limestones, and (3) the probable presence of some form of fluorapatite in limestones.

## ORGANIC GEOCHEMISTRY

### Introduction

Site 877 was drilled on the inner perimeter ridge of Wodejebato Guyot. According to the "Lithostratigraphy" section (this chapter), the type of rocks encountered at the site included manganese crust (Unit I); platform limestone (Unit II); clay, claystone, and claystone breccia (Unit III); and volcanic breccia (Unit IV).

The analytical program for Hole 877A included safety monitoring for hydrocarbon gases and chemical analyses of limestone and clay. Fifty-one samples were analyzed for inorganic carbon (IC), total organic carbon (TOC), nitrogen (N), and total sulfur (TS). Moreover, four samples were analyzed for organic matter type by pyrolysis. The procedures used for the analytical program are described in the "Organic Geochemistry" section of the "Explanatory Notes" chapter (this volume).

Lithologic Unit III was considered the most promising for organic geochemical investigations, and detailed sampling was performed on this unit. The unit included four lithofacies: bioturbated argillaceous grainstone with sand-sized shell fragments (Facies A); laminated, black clay, rich in plant remains and pyrite (Facies B); light gray, homogeneous clay with remains of plant roots (Facies C); and blue-green to red clay and claystone with relic structures of weathered volcaniclastic breccia (Facies D).

Although some intercalation between Facies A and B was observed in particular, the four facies corresponded to the following intervals of Unit III in general: Facies A = Interval 144-877A-20R-1, 0–77 cm; Facies B = Sections 144-877A-20R-1, 77 cm, to -20R-2,

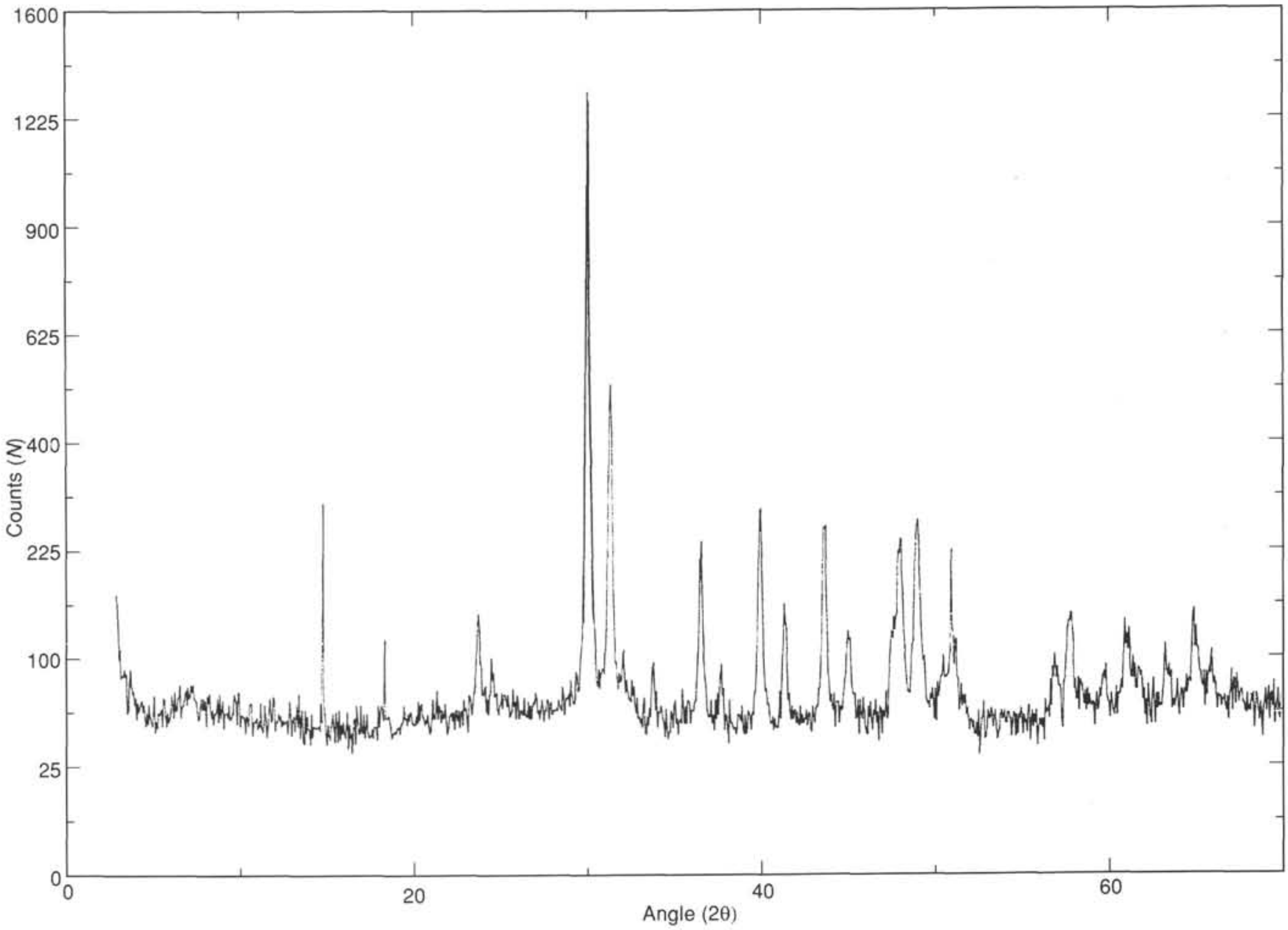


Figure 18. X-ray diffraction analysis of Sample 144-877A-3R-1, 57–64 cm. Calcite peak (1267 counts) occurs at an angle of 29.48°; dolomite peak (493 counts) occurs at an angle of 30.78°.

**Table 6. Results of headspace gas analyses, Site 877.**

| Sample identification | Methane (ppm) | Ethane (ppm) | Propane (ppm) | Lithology |
|---|---|---|---|---|
| 144-877A-20R-4, 0–5 cm | 2.0 | None | None | Red claystone |
| Laboratory background | 2.2 | None | None | |
| Core deck background | 1.8 | None | None | |
| Sea air background | 1.8 | None | None | |

Note: None = no gas detected.

35 cm; Facies C = Interval 144-877A-20R-2, 35–110 cm; and Facies D = Sections 144-877A-20R-2, 110 cm, to -20R-4, 100 cm.

## Volatile Hydrocarbons

The shipboard safety and pollution monitoring program requires the measurement of light hydrocarbon gases ($C_1$ to $C_3$) in cores immediately after retrieval onto the core deck. At Site 877, one headspace gas sample was obtained from the red claystone (Lithologic Unit III). The results of the analysis are given in Table 6. Methane concentration (2.0 ppm) was at the same level as the laboratory background. The very low light gas concentration can be ascribed to low concentrations of organic carbon in the red claystone (TOC below 0.8%). Light hydrocarbon gases were not considered a safety hazard at this site.

## Carbonate Carbon

Inorganic carbon (IC) content was measured in 51 samples with the Coulometrics carbon dioxide coulometer and reported as weight percent calcium carbonate. Sampling was performed in a way to obtain representative material with regard to both lithotypes and depth. Twenty-nine microsamples from the limestone in Lithologic Unit II (approximately 100 mg each) were collected by hand-drilling using a standard 5-mm drill bit. Twenty-one samples of the clay and argillaceous limestone in Lithologic Unit III were collected directly from the split core. One sample was taken from the volcaniclastic materials in Unit IV. Results of the inorganic carbon analyses are given in Tables 7 and 8, and carbonate data are shown in Figure 19.

Carbonate content was high in all samples from the platform limestone in Cores 144-877A-1R through -19R (Lithologic Unit II, average $CaCO_3$ = 98.1%). No significant difference in carbonate content was found between the calcareous lithotypes.

The boundary between Lithologic Units II and III was marked by a decline in carbonate content smaller than the one observed at Site 874. $CaCO_3$ values dropped from 98% in Core 144-877A-19R, to 68% in the argillaceous grainstone at the top of Core 144-877A-20R. At this level (Interval 144-877A-20R-1, 10–77 cm), alternating beds of carbonate-rich argillaceous limestone of

Facies A and carbonate-poor black clay of Facies B were observed, forming at least three upward-coarsening cycles.

The black, gray, and red clay of Facies B, C, and D contained <1% calcium carbonate. Slightly higher carbonate contents (1.6%) were observed in the weathered volcanic breccia of Lithologic Unit IV.

## Organic Carbon and Total Sulfur

Contents of total carbon (TC), nitrogen (N), and total sulfur (TS) were determined using the Carlo Erba Model NA1500 elemental analyzer. Total organic carbon (TOC) values were calculated from the difference between TC and IC. Detection limits for TOC, N, and TS were 0.1%, 0.02%, and 0.02%, respectively. Analyses were performed on the 51 samples used for carbonate carbon determinations. The results of the TOC, N, and TS analyses are given in Tables 7–8 and in Figures 19–21.

Very low TOC values were found in the platform limestone from Lithologic Unit II (average TOC < 0.1%). In the same unit, nitrogen and sulfur were below detection limit. In Lithologic Unit III, TOC and TS values showed large variations (Fig. 20). In general, Facies A (argillaceous grainstone) was low in organic carbon (average TOC = 1.3%) and rich in sulfur (average TS = 7.9%); Facies B (black clay) was very rich in both organic carbon and sulfur (average TOC = 17.0%, average TS = 18.8%); Facies C (gray clay) was very low in organic carbon (average TOC = 0.5%) and rich in sulfur (average TS = 12.9%); and Facies D (gray and red clay and claystone) was low in organic carbon (average TOC < 0.6%) and very rich to low in sulfur (average TS in gray clay: 12.9%, average TS in red clay: 0.3%). Most of the sulfur occurred as pyrite and marcasite, but considerable enrichments of organic sulfur cannot be excluded. Other sulfur-bearing minerals were not observed. Nitrogen was very low except in Facies B, where values up to 0.25% were measured. Organic carbon and nitrogen were highly correlated in this facies (Fig. 21). The TS/TOC ratios were above 1, except in three samples from Facies B, and reached values in excess of 100 in samples low in organic carbon (Fig. 21).

The very high TOC and TC values encountered in Facies B are remarkable. In some of the samples, organic matter and pyrite constituted more than 60% of the rock. After drying, these samples could burn when ignited. The samples represent the highest TOC and TS values hitherto observed on Legs 143 and 144.

**Table 7. Results of geochemical analyses, Hole 877A.**

| Core, section, interval (cm) | Depth (mbsf) | IC (wt%) | $CaCO_3$ (wt%) | TC (wt%) | TOC (wt%) | N (wt%) | TS (wt%) | Lithology |
|---|---|---|---|---|---|---|---|---|
| 144-877A- | | | | | | | | |
| 1R-1, 55–57 | 0.55 | 11.81 | 98.38 | 11.76 | 0 | 0 | 0 | Packstone |
| 1R-1, 137–139 | 1.37 | 11.76 | 97.96 | 11.90 | 0.14 | 0.01 | 0 | Framestone |
| 1R-2, 73–75 | 2.21 | 11.88 | 98.96 | 11.88 | 0 | 0 | 0.01 | Packstone |
| 1R-2, 104–107 | 2.52 | 11.81 | 98.38 | 11.87 | 0.06 | 0.01 | 0 | Packstone |
| 2R-1, 47–49 | 9.97 | 11.41 | 95.05 | 12.01 | 0.60 | 0 | 0 | Grainstone |
| 3R-1, 36–38 | 19.36 | 12.21 | 101.71 | 12.32 | 0.10 | 0.01 | 0.01 | Wackestone |
| 3R-1, 106–109 | 20.06 | 11.72 | 97.63 | 11.92 | 0.20 | 0 | 0 | Packstone |
| 4R-1, 32–39 | 28.72 | 11.79 | 98.21 | 11.65 | 0 | 0 | 0 | Packstone |
| 4R-2, 14–17 | 30.05 | 11.76 | 97.96 | 11.80 | 0.04 | 0.02 | 0 | Rudstone |
| 4R-2, 134–136 | 31.25 | 11.88 | 98.96 | 11.83 | 0 | 0 | 0 | Rudstone |
| 4R-3, 46–49 | 31.87 | 11.81 | 98.38 | 11.79 | 0 | 0.01 | 0 | Rudstone |
| 5R-1, 73–76 | 38.73 | 11.76 | 97.96 | 11.87 | 0.11 | 0.01 | 0.46 | Grainstone |
| 5R-2, 80–83 | 40.24 | 11.76 | 97.96 | 11.63 | 0 | 0.01 | 0 | Grainstone |
| 5R-3, 66–71 | 41.61 | 11.74 | 97.79 | 12.01 | 0.27 | 0.01 | 0 | Rudstone |
| 5R-3, 93–96 | 41.88 | 11.81 | 98.38 | 11.84 | 0.03 | 0.01 | 0 | Rudstone |
| 6R-1, 78–81 | 48.38 | 11.76 | 97.96 | 11.75 | 0 | 0.01 | 0 | Boundstone |
| 7R-1, 58–61 | 57.88 | 11.77 | 98.04 | 11.75 | 0 | 0.01 | 0 | Grainstone |
| 8R-2, 47–51 | 59.27 | 11.77 | 98.00 | 11.91 | 0.14 | 0.01 | 0 | Boundstone |
| 9R-1, 12–19 | 76.72 | 11.71 | 97.54 | 11.66 | 0 | 0.01 | 0 | Grainstone |
| 10R-1, 13–17 | 86.43 | 11.71 | 97.54 | 11.31 | 0 | 0.01 | 0.01 | Boundstone |
| 12R-1, 17–23 | 105.87 | 11.83 | 98.50 | 11.59 | 0 | 0 | 0 | Grainstone |
| 13R-1, 1–6 | 115.31 | 11.68 | 97.29 | 11.75 | 0.07 | 0.01 | 0 | Grainstone |
| 14R-1, 20–22 | 125.20 | 11.81 | 98.38 | 11.42 | 0 | 0 | 0 | Grainstone |
| 14R-2, 120–127 | 126.20 | 11.81 | 98.38 | 11.80 | 0 | 0.01 | 0 | Grainstone |
| 15R-1, 0–4 | 134.60 | 11.86 | 98.79 | 11.33 | 0 | 0.01 | 0.01 | Grainstone |
| 16R-1, 57–68 | 144.87 | 11.87 | 98.88 | 11.50 | 0 | 0 | 0 | Grainstone |
| 17R-1, 0–10 | 153.90 | 11.69 | 97.38 | 11.15 | 0 | 0 | 0 | Grainstone |
| 18R-1, 4–6 | 163.54 | 11.78 | 98.13 | 11.27 | 0 | 0 | 0 | Grainstone |
| 19R-1, 13–18 | 173.33 | 11.73 | 97.71 | 12.03 | 0.30 | 0 | 0 | Packstone |
| 20R-1, 16–17 | 182.86 | 8.15 | 67.89 | 8.87 | 0.72 | 0.02 | 4.75 | Grainstone |
| 20R-1, 28–29 | 182.98 | 0.03 | 0.25 | 4.16 | 4.13 | 0.05 | 15.44 | Black clay |
| 20R-1, 42–44 | 183.12 | 5.77 | 48.06 | 6.80 | 1.03 | 0.04 | 7.42 | Grainstone |
| 20R-1, 44–45 | 183.14 | 4.51 | 37.57 | 6.29 | 1.78 | 0.04 | 9.36 | Grainstone |
| 20R-1, 54–55 | 183.24 | 4.13 | 34.40 | 6.93 | 2.80 | 0.04 | 10.31 | Grainstone |
| 20R-1, 70–71 | 183.40 | 6.72 | 55.98 | 7.01 | 0.29 | 0.02 | 7.78 | Packstone |
| 20R-1, 81–82 | 183.51 | 0.06 | 0.50 | 19.02 | 18.96 | 0.15 | 14.37 | Black peaty clay |
| 20R-1, 92–94 | 183.62 | 0.03 | 0.25 | 36.54 | 36.51 | 0.25 | 9.97 | Black peaty clay |
| 20R-1, 101–102 | 183.71 | 0.03 | 0.25 | 21.88 | 21.85 | 0.17 | 20.96 | Black peaty clay |
| 20R-2, 1–2 | 183.76 | 0.02 | 0.17 | 15.97 | 15.95 | 0.14 | 25.19 | Black peaty clay |
| 20R-2, 15–16 | 183.90 | 0.04 | 0.33 | 12.67 | 12.63 | 0.11 | 22.94 | Black peaty clay |
| 20R-2, 34–35 | 184.09 | 0.04 | 0.33 | 8.80 | 8.76 | 0.10 | 22.52 | Black peaty clay |
| 20R-2, 61–62 | 184.36 | 0.09 | 0.75 | 1.01 | 0.92 | 0.01 | 6.72 | Gray clay |
| 20R-2, 98–99 | 184.73 | 0.03 | 0.25 | 1.09 | 1.06 | 0.01 | 18.59 | Gray clay |
| 20R-2, 126–127 | 185.01 | 0.04 | 0.33 | 0.15 | 0.11 | 0 | 23.03 | Gray clay |
| 20R-3, 9–10 | 185.36 | 0.04 | 0.33 | 0.14 | 0.10 | 0 | 13.65 | Gray clay |
| 20R-3, 39–40 | 185.66 | 0.06 | 0.50 | 0.54 | 0.48 | 0 | 13.65 | Gray clay |
| 20R-3, 79–80 | 186.06 | 0.04 | 0.33 | 0.55 | 0.51 | 0 | 1.70 | Gray clay |
| 20R-3, 99–100 | 186.26 | 0.04 | 0.33 | 0.80 | 0.76 | 0 | 0.13 | Red clay |
| 20R-3, 134–135 | 186.61 | 0.03 | 0.25 | 0.08 | 0.05 | 0 | 0.73 | Red clay |
| 20R-3, 140–150 | 186.67 | 0.11 | 0.92 | 0.18 | 0.07 | 0 | 0.11 | Red clay |
| 20R-4, 75–76 | 187.52 | 0.19 | 1.60 | 0 | 0.09 | 0 | 0 | Volcanic breccia |

Notes: IC = inorganic carbon, $CaCO_3$ = carbonate carbon calculated as calcium carbonate, TC = total carbon, TOC = total organic carbon, N = nitrogen, and TS = total sulfur. All numbers are in weight percent.

**Table 8. Averages of geochemical results from Hole 877A.**

| Lithologic units | CaCO3 (wt%) | TOC (wt%) | N (wt%) | S (wt%) | General lithology |
|---|---|---|---|---|---|
| II | | | | | Limestone |
| Average | 98.10 | 0.07 | 0.01 | 0.02 | |
| SD | 1.00 | 0.13 | 0.01 | 0.09 | |
| *N* | 29 | 29 | 29 | 29 | |
| III | | | | | Muddy grainstone |
| Average | 48.86 | 1.32 | 0.03 | 7.92 | |
| SD | 13.69 | 0.99 | 0.01 | 2.13 | |
| *N* | 5 | 5 | 5 | 5 | |
| III | | | | | Black peaty clay |
| Average | 0.30 | 16.99 | 0.14 | 18.77 | |
| SD | 0.10 | 10.50 | 0.06 | 5.56 | |
| *N* | 7 | 7 | 7 | 7 | |
| III | | | | | Gray clay |
| Average | 0.41 | 0.53 | 0 | 12.89 | |
| SD | 0.18 | 0.40 | 0 | 7.74 | |
| *N* | 6 | 6 | 6 | 6 | |
| III | | | | | Red clay |
| Average | 0.50 | 0.29 | 0 | 0.32 | |
| SD | 0.37 | 0.40 | 0 | 0.35 | |
| *N* | 3 | 3 | 3 | 3 | |

Note: SD = standard deviation and *N* = number of samples.

## Organic Matter Type and Thermal Maturation Level

Shipboard geochemical characterization of organic matter is normally performed by Rock-Eval (RE) analysis and pyrolysis gas chromatography (Py-GC). Only samples containing more than 1% organic matter are considered suitable for these types of analyses. During the time spent at Site 877, the Rock-Eval instrument did not function, and organic matter characterization was performed by the Geofina instrument. This instrument provided reliable pyrolysis data ($S_1$, $S_2$, and $T_{max}$) for Site 877 but failed to produce Py-GC analyses.

Four samples from Lithologic Unit III in Hole 877A (Sample 144-877A-20R-1, 28–29 cm, from Facies B; Sample 144-877A-20R-1, 54–55 cm, from Facies A; Sample 144-877A-20R-1, 92–94 cm, from Facies B; and Sample 144-877A-20R-2, 15–16 cm, from Facies B) were analyzed by the Geofina pyrolysis instrument. Results are reported in Table 9 and in Figure 22. Organic matter from the argillaceous limestone and the intercalated black clay contained very small amounts of free or pyrolyzable hydrocarbons and belonged to a type III to IV ("woody" to "inert") kerogen. Organic matter from the black, peaty clay below the limestone was slightly richer in pyrolyzable hydrocarbons and could be characterized as a "true" type III kerogen. Optical inspection demonstrated woody material to be the dominant visual organic phase (see "Biostratigraphy" section, this chapter). Thermal maturity corresponded to immature conditions, as seen from the low $T_{max}$ and hydrogen index (HI) values. The variation in $T_{max}$ values can be ascribed to varying amounts of organically bound sulfur in the kerogen.

## Interpretation of Organic Facies and Depositional Environments

Three major depositional environments are represented at Site 877: (1) shallow-water, open marine (represented by the platform limestone in Lithologic Unit II); (2) shallow-water, restricted marine (represented by Facies A and B in Unit III); and (3) terrestrial (represented by Facies C and D in Unit III).

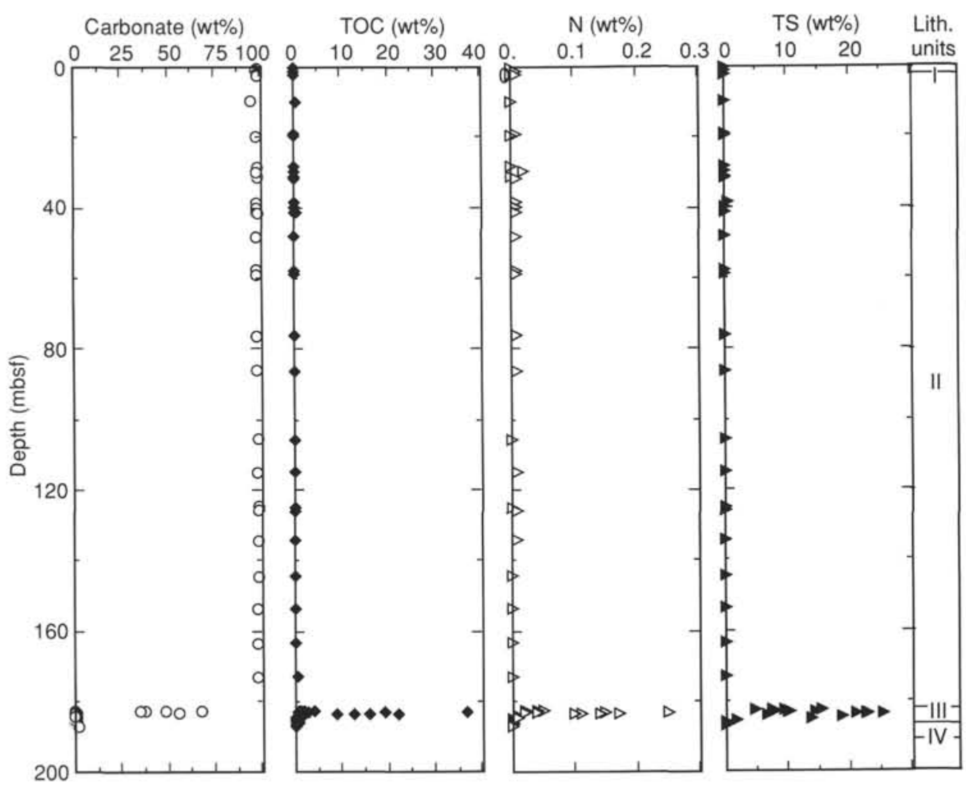


Figure 19. Carbonate (calculated as weight percent calcium carbonate), total organic carbon (TOC), nitrogen (N), and total sulfur (TS) contents of sediments in Hole 877A. Also shown are the major lithologic units, as given in the "Lithostratigraphy" section (this chapter).

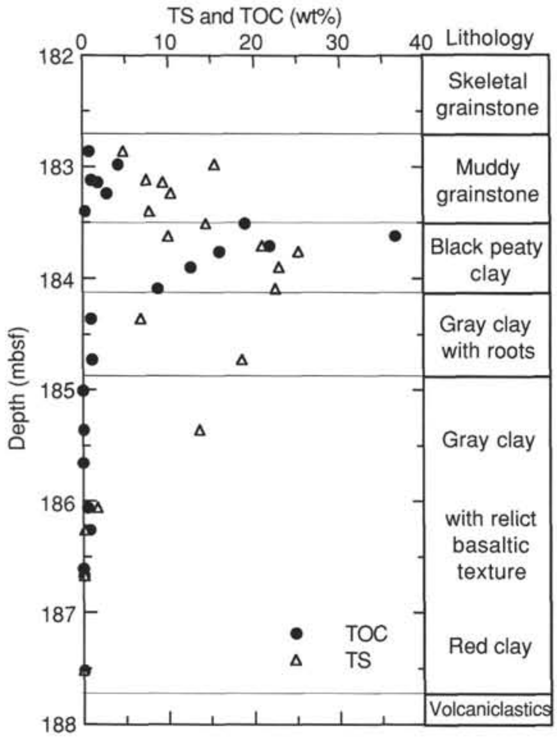


Figure 20. Total sulfur (TS) and total organic carbon (TOC) content for the transition from limestone to clay in Hole 877A. Note the high sulfur content in the units low in organic carbon.

In the open-marine, shallow-water environment, preservation of organic matter was extremely poor. The TOC values below 0.3% in all but one sample and TS values below the detection limit indicate deposition under oxic conditions with very low preservation potential for organic matter. Most of the organic matter probably was of marine origin.

In the restricted-marine, shallow-water environment, preservation of organic matter was highly favorable, especially in the black clay of Facies B. The very high content of pyritic sulfur must be a result of intense bacterial sulfate reduction under subaquatic, anoxic conditions, with seawater as sulfate source. The intensive sulfate reduction most probably took place in the organic-rich black clay of Facies B, and hydrogen sulfide diffusing from there into the adjacent facies was precipitated as iron sulfides. Organic matter necessary for the sulfate reduction was provided by influx from terrestrial sources and from the local growth of algae and bacteria. However, because of the intensive bacterial degradation of the initial organic material, only refractive organic matter of woody composition low in hydrogen and nitrogen remain in the clay.

It is not clear whether the black, peaty clay of Facies B originally was deposited under marine or nonmarine conditions. The occurrence of a well-developed root horizon in Facies C immediately below the lowest occurrence of black clay indicates a nonmarine environment, whereas the intense sulfate reduction demonstrates influx of seawater. Most probably, the black clay represents the transitional facies between nonmarine and marine conditions and thus marks the initial marine transgression at Site 877. Nannofossils from the argillaceous limestone immediately above the black clay (Sample 144-877A-20R-1, 44–45 cm) yield a late Campanian age for this transgression (see "Biostratigraphy" section, this chapter).

## Conclusions

No volatile hydrocarbons were encountered at this site. Organic matter at this site is thermally immature with regard to hydrocarbon formation.

The platform limestone (Lithologic Unit II) had calcium carbonate contents from 97% to 100%. Only very low concentrations of organic matter were encountered. The unit was deposited under oxic conditions.

The black, peaty clay in Lithologic Unit III was deposited under anoxic conditions and was affected by intense bacterial sulfate reduction. The facies represents the highest enrichments in sulfur and organic carbon encountered on Leg 144. The organic matter in the black, peaty clay, as found today, has a composition corresponding to a type III (woody) kerogen of terrestrial origin.

The black, peaty clay and argillaceous limestone in Lithologic Unit III mark the initial marine transgression at the site. The nannofossils present in the limestone date this event as late Campanian age. The high sulfur content of the gray, terrestrial clay and weathered volcaniclastic materials below the black clay reflects downward diffusion of reducing, hydrogen-sulfide-rich fluids. The boundary between the gray and red clay represents the reduction front.

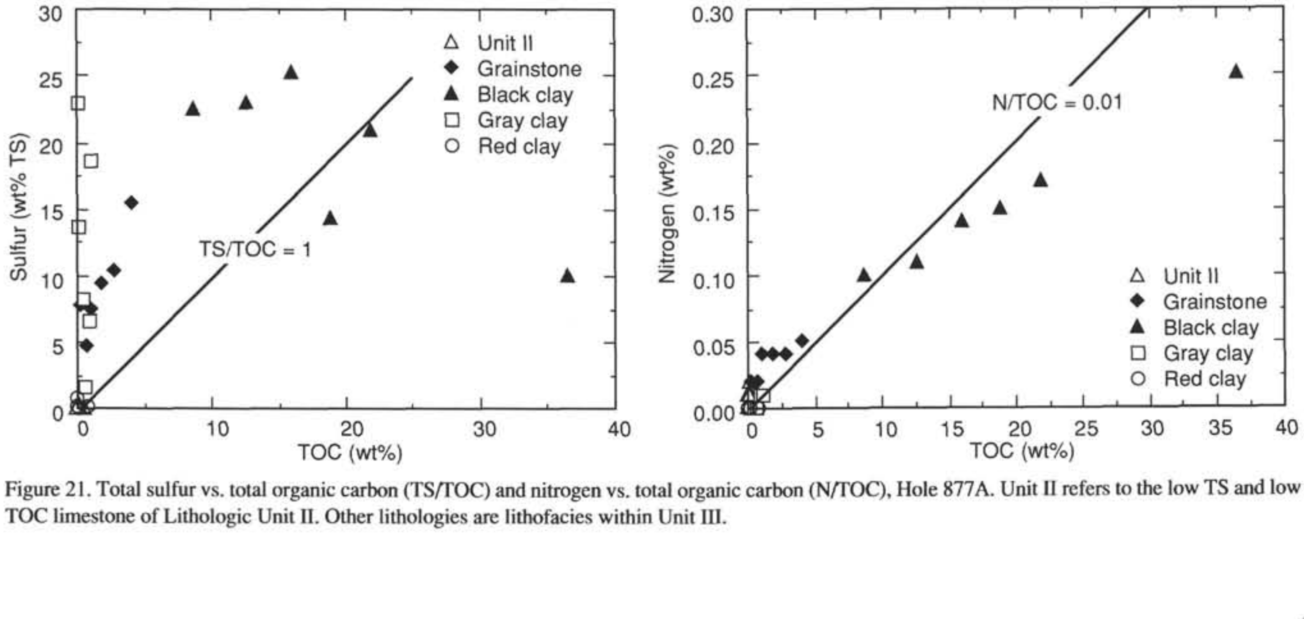


Figure 21. Total sulfur vs. total organic carbon (TS/TOC) and nitrogen vs. total organic carbon (N/TOC), Hole 877A. Unit II refers to the low TS and low TOC limestone of Lithologic Unit II. Other lithologies are lithofacies within Unit III.

**Table 9. Results of the pyrolysis analyses of organic-rich samples from Hole 877A obtained by means of the Geofina hydrocarbon meter.**

| Core, section, interval (cm) | TOC (wt%) | S1 (mg/g) | S1/TOC | S2 (mg/g) | HI (mg/g) | PI | $T_{max}$ | Lithology |
|---|---|---|---|---|---|---|---|---|
| 144-877A- | | | | | | | | |
| 20R-1, 28–29 | 4.13 | 0.45 | 0.11 | 2.63 | 64 | 0.15 | 407 | Black clay |
| 20R-1, 54–55 | 2.80 | 0.22 | 0.08 | 1.89 | 67 | 0.11 | 410 | Muddy grainstone |
| 20R-1, 92–94 | 36.51 | 0.24 | 0.01 | 43.98 | 120 | 0.01 | 423 | Black peaty clay |
| 20R-2, 15–16 | 12.63 | 0.33 | 0.03 | 18.90 | 150 | 0.02 | 410 | Black clay |

Notes: TOC = total organic carbon, from Table 7; S1 and S2 = mg hydrocarbon/gram of rock, HI = hydrogen index (mg hydrocarbon/gram of organic carbon), PI = production index (free hydrocarbon relative to total hydrocarbon), and $T_{max}$ = maximal S2 pyrolysis temperature (in degrees Celsius). Further explanation of the pyrolysis parameters are given in the "Organic Geochemistry" section, "Explanatory Notes" chapter (this volume).

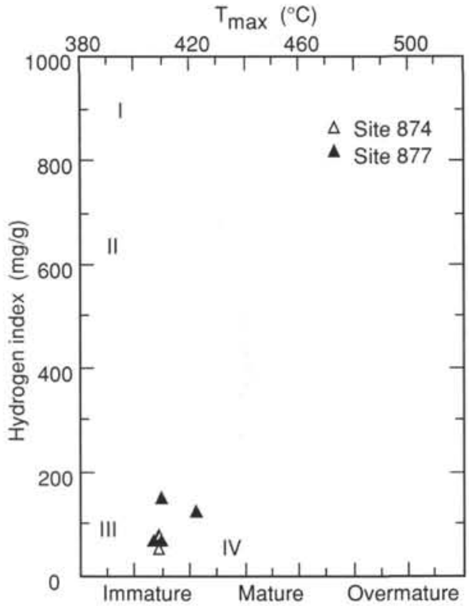


Figure 22. Kerogen typing and thermal maturation for organic matter from Hole 877A. Samples are from the organic-rich argillaceous limestone and black, peaty clay in Lithologic Unit III. Also shown are data from Site 874. Roman numerals refer to kerogen types: type I is algal, type II is algal/herbaceous, type III is woody, and type IV is highly oxidized. The investigated

## IGNEOUS PETROLOGY

### Introduction

Site 877 was drilled on the inner perimeter ridge near the northern edge of Wodejebato Guyot. In Hole 877A, basalt breccia (Lithologic Unit IV) was reached at 189.7 mbsf, and 76 cm of the breccia were recovered. The breccia occurs beneath and in contact with 4.3 m of claystone (Lithologic Unit III: Sections 144-877A-20R-1, 77 cm, through -20R-4, 98 cm), which clearly retains the fabric of the underlying basalt breccia through much of its thickness. The claystone represents an in-situ, presumably subaerial, weathering profile developed on the breccia.

### Hole 877A

The basaltic breccia of Lithologic Unit IV (Sections 144-877A-20R-4, 98 cm, through -20R-5, 35 cm) contains 0.5- to 3.0-cm clasts of vesicular, plagioclase-clinopyroxene basalt. The clast outlines are barely distinguishable, and they have a clay and calcite matrix. The clasts contain up to 10% irregular vesicles, <3 mm in diameter, filled with green clay. In Interval 144-877A-20R-4, 122–130 cm, calcite occurs in thin (0.5–7.0 mm thick), anastomosing, subhorizontal veins that replace up to 50% of the breccia.

In thin section, the clasts have <3% fractured, rounded, pale green clinopyroxene grains, 1–4 mm in diameter, with skeletal quench overgrowths along their edges, and 5%–15% prismatic or broken and rounded plagioclase grains, <2 mm in diameter, with irregular extinction patterns, perhaps as the result of deformation. Clinopyroxene and plagioclase often occur together as glomerocrysts, which appear to be xenocrysts because of the broken, rounded shapes and irregular extinction patterns. The groundmass has 20%–30% fresh, swallow-tailed plagioclase, <0.2 mm in diameter, in a hydrated glass matrix. Hydration and replacement by green and brown clay has destroyed over half of the original plagioclase and glass.

### Summary

Below a thick, subaerial, in-situ, claystone-weathering profile, solid breccia was reached at 189.7 mbsf. The presence of the claystone indicates that the transition from subaerial to marine conditions took place in a low-energy environment. The breccia clasts are vesicular basalt containing clinopyroxene and plagioclase xenocrysts and plagioclase microlites in a hydrated glass matrix. The groundmass has been extensively replaced by green and brown clays.

## PHYSICAL PROPERTIES

### Introduction

The objectives of the physical properties measurement program at Site 877 were (1) to measure the standard shipboard physical properties and (2) to identify geotechnical units for downhole and cross-hole correlations. The standard shipboard physical properties program included (1) measurements of magnetic susceptibility, made using a sensor mounted on the multisensor track (MST) and (2) discrete measurements of index properties and compressional wave velocity (see "Explanatory Notes" chapter, this volume). Compressional wave velocities were measured using the Hamilton Frame (HF) on sample cubes and cylinders (minicores) of limestone and basalt. No thermal conductivity measurements were made because of malfunctioning equipment.

Hard-rock cores were obtained in Hole 877A using the rotary core barrel (RCB), but recovery was very poor. A total of 182.9 m of limestone, 4.3 m of clays, and 1.6 m of volcanic breccia were drilled. Whole-round core sections of limestone, basalt, and clay were passed through the MST-mounted magnetic susceptibility sensor before they were split; shipboard and shore-based whole-round samples were cut first from either end of the section.

Samples recovered in Hole 877A consist of algal and skeletal limestones from 0 to 182.9 mbsf, clays and argillaceous limestones from 182.9 to 187.2 mbsf, and volcanic breccia from 187.2 to 190.5 mbsf. The limestones consist of white, highly porous, skeletal grainstone; skeletal fenestral wackestone; and algal rudist rudstone; all limestones are Maastrichtian in age. The limestone is capped by a thin algal rudist boundstone encrusted with manganese (Paleocene to middle Eocene age).

Test data are given in Tables 10 and 11 (See "Paleomagnetism" section, this chapter, for magnetic susceptibility data).

### Physical Properties Units

*Limestone*

The limestones may be tentatively divided into three geotechnical subunits: Subunit 1A (0–105.5 mbsf) encompassing Lithologic Subunits IIA, IIB, and IIC (0.3–105.7 mbsf); Subunit 1B (105.5–150 mbsf approximately) containing the upper part of Lithologic Subunit IID; Subunit 1C (150–182.9 mbsf) containing the lower part of Lithologic Subunit IID and the whole of Lithologic Subunit IIE. The boundary between Geotechnical Subunits 1B and 1C is not clearly defined because of a lack of data; it may be gradational (Fig. 23). The compressional wave velocity data (Fig. 24) do not fit with this unit selection (which is based on changes in index properties). The contrast in index properties between Geotechnical Subunits 1A and 1B is most striking, particularly in relation to the porosity.

For Geotechnical Subunit 1A, dry-bulk density ranges from 2.62 to 2.93 g/cm$^3$, with a mean of 2.75 g/cm$^3$. In the case of Subunit 1B, dry-bulk density ranges from 1.52 to 1.95 g/cm$^3$, with a mean of 1.71 g/cm$^3$. Porosities in Subunit 1A range from 2.0% to 11.9%, with a mean of 5.13%. This compares with a range of 32.8% to 52.7% and a mean of 44.0% for Subunit 1B. For Subunit 1C, dry-bulk density results range from 2.08 to 2.71 g/cm$^3$, with a mean of 2.41 g/cm$^3$; porosity results range from 10.6% to 30.70%, with a mean of 19.4%.

The compressional wave velocity data for Geotechnical Subunit 1A range from 4804 to 5915 m/s, with a mean of 5270 m/s. The one sample from Subunit 1B yielded velocity values of 1951, 1981, and 2068 m/s for each of the three measurement axes. For Subunit 1C, velocity ranges from 3244 to 4800 m/s, with a mean of 3681 m/s. Compressional wave velocity signal strengths for all measurements of Unit 1 limestones are poor or very poor.

### *Clay*

The clays and argillaceous limestones are represented by Geotechnical Unit 2 (182.9–187.2 mbsf), which is equivalent to Lithologic Unit III. Dry-bulk density ranges from 0.8 to 1.6 g/cm$^3$, with a mean of 1.31 g/cm$^3$. Porosity ranges from 50.7% to 68.4%, with a mean of 58.2%. Compressional wave velocities were not determined for this unit because of the unsuitability of the test methods in these materials. Index property values in this unit show considerable scatter because of the lithologic variability.

**Table 10. Index properties data, Hole 877A.**

| Core, section, interval (cm) | Depth (mbsf) | Wet-bulk density (g/cm$^3$) | Dry-bulk density (g/cm$^3$) | Grain density (g/cm$^3$) | Porosity (%) | Water content (% dry wt) | Void ratio |
|---|---|---|---|---|---|---|---|
| 144-877A- | | | | | | | |
| 1R-1, 55–57 | 0.55 | 2.79 | 2.74 | 2.77 | 4.8 | 1.8 | 0.05 |
| 1R-1, 137–139 | 1.37 | 2.90 | 2.85 | 2.76 | 4.6 | 1.7 | 0.05 |
| 1R-2, 73–75 | 2.21 | 2.80 | 2.72 | 2.78 | 8.0 | 3.0 | 0.09 |
| 1R-2, 104–106 | 2.52 | 2.76 | 2.73 | 2.70 | 3.3 | 1.3 | 0.03 |
| 2R-1, 47–49 | 9.97 | 2.81 | 2.74 | 2.76 | 7.1 | 2.7 | 0.08 |
| 3R-1, 36–38 | 19.36 | 2.79 | 2.67 | 2.83 | 11.9 | 4.6 | 0.14 |
| 3R-1, 106–108 | 20.06 | 2.83 | 2.81 | 2.72 | 2.5 | 0.9 | 0.03 |
| 4R-1, 32–34 | 28.72 | 2.72 | 2.68 | 2.72 | 3.7 | 1.4 | 0.04 |
| 4R-2, 14–16 | 30.05 | 2.77 | 2.74 | 2.71 | 2.6 | 1.0 | 0.03 |
| 4R-2, 134–136 | 31.25 | 2.85 | 2.78 | 2.73 | 6.5 | 2.4 | 0.07 |
| 4R-3, 46–48 | 31.87 | 2.80 | 2.76 | 2.70 | 3.9 | 1.5 | 0.04 |
| 5R-1, 73–76 | 38.73 | 2.78 | 2.71 | 2.65 | 6.5 | 2.5 | 0.07 |
| 5R-2, 80–83 | 40.24 | 2.76 | 2.71 | 2.69 | 5.0 | 1.9 | 0.05 |
| 5R-3, 66–71 | 41.61 | 2.77 | 2.73 | 2.70 | 4.4 | 1.6 | 0.05 |
| 5R-3, 93–96 | 41.88 | 2.95 | 2.93 | 2.78 | 2.0 | 0.7 | 0.02 |
| 6R-1, 78–81 | 48.38 | 2.83 | 2.79 | 2.68 | 4.1 | 1.5 | 0.04 |
| 7R-1, 58–61 | 57.88 | 2.79 | 2.76 | 2.67 | 3.1 | 1.1 | 0.03 |
| 7R-2, 109–120 | 59.89 | 2.70 | 2.62 | 2.70 | 8.4 | 3.3 | 0.09 |
| 8R-1, 47–51 | 67.47 | 2.87 | 2.83 | 2.70 | 3.6 | 1.3 | 0.04 |
| 12R-1, 17–23 | 105.87 | 2.07 | 1.60 | 2.93 | 46.2 | 29.6 | 0.86 |
| 14R-1, 20–22 | 125.20 | 2.06 | 1.52 | 2.83 | 52.7 | 35.5 | 1.11 |
| 14R-2, 120–127 | 127.70 | 2.13 | 1.68 | 2.74 | 43.8 | 26.7 | 0.78 |
| 15R-1, 0.1–4 | 134.60 | 2.26 | 1.81 | 2.78 | 44.3 | 25.2 | 0.80 |
| 16R-1, 57–68 | 144.87 | 2.29 | 1.95 | 2.78 | 32.8 | 17.2 | 0.49 |
| 17R-1, 7–10 | 153.97 | 2.81 | 2.71 | 2.78 | 10.6 | 4.0 | 0.12 |
| 18R-1, 4–6 | 163.54 | 2.39 | 2.08 | 2.80 | 30.7 | 15.1 | 0.44 |
| 19R-1, 13–18 | 173.33 | 2.60 | 2.43 | 2.79 | 16.9 | 7.2 | 0.20 |
| 20R-1, 45–47 | 183.15 | 2.12 | 1.60 | 3.00 | 50.7 | 32.5 | 1.03 |
| 20R-1, 88–89 | 183.58 | 1.50 | 0.80 | 2.08 | 68.4 | 87.3 | 2.16 |
| 20R-2, 64–65 | 184.39 | 2.08 | 1.52 | 3.14 | 54.1 | 36.4 | 1.18 |
| 20R-3, 39–41 | 185.66 | 2.06 | 1.52 | 3.01 | 53.3 | 36.0 | 1.14 |
| 20R-3, 113–114 | 186.40 | 1.78 | 1.12 | 2.99 | 64.3 | 58.7 | 1.80 |
| 20R-4, 74–76 | 187.51 | 1.91 | 1.33 | 2.88 | 56.3 | 43.2 | 1.29 |
| 20R-4, 120–122 | 187.97 | 2.58 | 2.31 | 2.82 | 26.2 | 11.6 | 0.36 |
| 20R-5, 14–16 | 188.32 | 2.80 | 2.60 | 3.01 | 19.5 | 7.7 | 0.24 |

### *Volcanic Breccia*

The volcanic breccia is represented by Geotechnical Unit 3 (187.2–190.5 mbsf), which is equivalent to Lithologic Unit IV. Dry-bulk density results are 1.33, 2.31, and 2.6 g/cm$^3$. Porosity results are 56.3%, 26.2%, and 19.5%. The sole compressional wave velocity measurement in this unit is 2940 m/s.

### Discussion

Index property and compressional wave velocity values measured on samples from Hole 877A show similar trends as those in Hole 874B ("Physical Properties" section, "Site 874" chapter, this volume). Contrasts from one geotechnical unit to the next are, if anything, stronger in the case of Hole 877A. The algal and foraminifer grainstones, packstones, and rudstones in both holes exhibit much lower porosity and higher densities than the skeletal grainstones and packstones. The clays in Holes 877A and 874B are seen to have very high porosity and low wet- and dry-bulk density values. Results from the basalts in the two holes show considerable scatter, but they lie in the same range as each other.

It is clear from the index properties of Geotechnical Subunit 1A that errors in the determinations of wet and dry volumes are considerable (as much as 5%) when small changes in volume are used in the calculations, as for example with the limestones of Subunit 1A. In many cases, the dry specimen volumes have been found to be greater than the wet specimen volumes, resulting in dry-bulk densities greater than grain densities. This is clearly incorrect. If wet porosity is then calculated using wet and dry volumes, the result is a negative number. However, the ODP index spreadsheet uses water weight and wet volume to calculate wet porosity, thus yielding positive values.

## DOWNHOLE MEASUREMENTS AND SEISMIC STRATIGRAPHY

### Drilling Penetration Rates and Implications for Lithostratigraphy

Downhole logging runs were not performed at Site 877 because of time constraints. However, drilling penetration rates in Hole 877A, which penetrated through the carbonate platform to the uppermost volcanics, provide a proxy for identifying changes in lithology and in cementation (Fig. 25). At other sites on Wodejebato Guyot, variations in penetration rates were observed to coincide with resistivity and density fluctuations and, therefore, may be related to porosity (e.g., Fig. 51, "Site 873" chapter, and Fig. 35, "Site 874" chapter, this volume). Major changes in drilling rates can be used (1) to assign boundaries among some major lithologic units (see "Lithostratigraphy" section, this chapter); (2) to identify possible facies characteristics that were not recovered during the coring; and (3) to locate the contact with the hard basaltic basement.

Drilling penetration rates were slow (30–100 min/m) within the hard manganese-encrusted surface and underlying 9 m of algal rudist boundstone (Lithologic Unit I and Subunit IIA). From 10 through 28 mbsf, corresponding to the skeletal fenestral wackestone to grainstone of Lithologic Subunit IIB, drilling penetration averaged about 15 min/m (Fig. 25).

Between 28 and 45 mbsf, penetration rates indicate three intervals of well-cemented material, which required 20–30 min of drilling per meter. Corresponding Cores 144-877A-4R and -5R contain intervals of densely cemented algal-rudist boundstone (upper portion of Lithologic Subunit IIC). We suggest, therefore, that the hard layers encountered in drilling represent intervals of

**Table 11. Hamilton Frame measurements of compressional wave velocity, Hole 877A.**

| Core, section, interval (cm) | Depth (mbsf) | Distance (mm) | Axes of measurement | Traveltime (μs) | Corrected traveltime (μs) | Measured velocity (m/s) | Velocity anistropy index |
|---|---|---|---|---|---|---|---|
| 144-877A- | | | | | | | |
| 1R-1, 55–57 | 0.55 | 17.76 | a | 6.53 | 3.53 | 5038.30 | |
| 1R-1, 55–57 | 0.55 | 21.60 | b | 7.05 | 4.05 | 5333.33 | |
| 1R-1, 55–57 | 0.55 | 22.29 | c | 7.45 | 4.45 | 5014.62 | 0.03 |
| 1R-2, 73–75 | 2.21 | 21.29 | a | 7.22 | 4.22 | 5051.01 | |
| 1R-2, 73–75 | 2.21 | 21.64 | b | 7.08 | 4.08 | 5303.92 | |
| 1R-2, 73–75 | 2.21 | 21.57 | c | 7.08 | 4.08 | 5293.25 | –0.02 |
| 3R-1, 33–35 | 19.33 | 22.68 | a | 7.38 | 4.38 | 5178.08 | |
| 3R-1, 33–35 | 19.33 | 21.76 | b | 7.14 | 4.14 | 5262.39 | |
| 3R-1, 33–35 | 19.33 | 21.58 | c | 7.21 | 4.21 | 5125.89 | 0.02 |
| 4R-2, 14–16 | 30.05 | 19.89 | a | 6.78 | 3.78 | 5261.91 | |
| 4R-2, 14–16 | 30.05 | 21.60 | b | 6.89 | 3.89 | 5559.85 | |
| 4R-2, 14–16 | 30.05 | 21.94 | c | 7.05 | 4.05 | 5423.98 | 0.00 |
| 4R-3, 47–49 | 31.88 | 21.57 | a | 7.26 | 4.26 | 5063.38 | |
| 4R-3, 47–49 | 31.88 | 21.71 | b | 6.87 | 3.87 | 5617.08 | |
| 4R-3, 47–49 | 31.88 | 21.92 | c | 7.30 | 4.30 | 5103.61 | 0.05 |
| 4R-3, 47–49 | 31.88 | 21.70 | a | 6.91 | 3.91 | 5549.87 | |
| 4R-3, 47–49 | 31.88 | 21.54 | b | 7.05 | 4.05 | 5318.52 | |
| 4R-3, 47–49 | 31.88 | 22.18 | c | 7.39 | 4.39 | 5052.39 | 0.07 |
| 5R-1, 73–76 | 38.73 | 21.49 | a | 7.02 | 4.02 | 5345.77 | |
| 5R-1, 73–76 | 38.73 | 23.51 | b | 7.33 | 4.33 | 5429.56 | |
| 5R-1, 73–76 | 38.73 | 21.50 | c | 7.02 | 4.02 | 5348.26 | 0.01 |
| 5R-2, 80–83 | 40.24 | 21.62 | a | 7.50 | 4.50 | 4804.44 | |
| 5R-2, 80–83 | 40.24 | 19.77 | b | 6.68 | 3.68 | 5372.28 | |
| 5R-2, 80–83 | 40.24 | 21.54 | c | 6.93 | 3.93 | 5480.92 | –0.07 |
| 5R-3, 59–61 | 41.54 | 22.06 | a | 7.19 | 4.19 | 5264.92 | |
| 6R-1, 78–81 | 48.38 | 22.20 | a | 6.99 | 3.99 | 5563.91 | |
| 6R-1, 78–81 | 48.38 | 21.56 | b | 6.78 | 3.78 | 5703.70 | |
| 6R-1, 78–81 | 48.38 | 21.65 | c | 6.66 | 3.66 | 5915.30 | –0.05 |
| 7R-2, 109–120 | 59.89 | 21.52 | a | 7.48 | 4.48 | 4803.57 | |
| 7R-2, 109–120 | 59.89 | 21.96 | b | 7.60 | 4.60 | 4773.91 | |
| 7R-2, 109–120 | 59.89 | 21.58 | c | 7.31 | 4.31 | 5006.96 | –0.04 |
| 14R-1, 20–22 | 125.20 | 21.01 | a | 13.77 | 10.77 | 1950.79 | |
| 14R-1, 20–22 | 125.20 | 21.18 | b | 13.69 | 10.69 | 1981.29 | |
| 14R-1, 20–22 | 125.20 | 20.74 | c | 13.03 | 10.03 | 2067.80 | –0.05 |
| 17R-1, 7–8 | 153.97 | 11.64 | c | 5.43 | 2.43 | 4800.00 | |
| 18R-1, 4–6 | 163.54 | 21.41 | a | 9.60 | 6.60 | 3243.94 | |
| 18R-1, 4–6 | 163.54 | 21.17 | b | 9.30 | 6.30 | 3360.32 | |
| 18R-1, 4–6 | 163.54 | 21.55 | c | 9.49 | 6.49 | 3320.49 | –0.01 |
| 20R-4, 120–121 | 187.97 | 13.17 | c | 7.48 | 4.48 | 2939.73 | |

Notes: a = direction perpendicular to split core plane, b = direction transverse to split core plane, and c = core axis; all axes are orthogonal.

reef facies. The thickest of these reef layers spans 7 m (38–45 mbsf). Overlying and maybe interspersed within these reef episodes are relatively less dense layers, which probably correspond to skeletal packstone-grainstone. Core 144-877A-3R may also contain a rudist reef at 23 mbsf, in addition to a thin-bedded lime mudstone of possible intertidal origin.

Below this rudist reefal facies are interbedded layers of relatively harder and softer carbonate. Recovery in Cores 144-877A-6R and -7R suggests that the harder layers correspond to the packstone-grainstone of rudist and shell debris with some red-algae-encrusted rudist rudstone and that the softer layers are poorly sorted rudstone.

Drilling penetration rates generally were faster than 3 min/m from 74 to 92 mbsf (base of Core 144-877A-8R to upper -10R), corresponding to a porous skeletal wackestone facies (lower Lithologic Subunit IIC).

From 92 to 150 mbsf, drilling penetration rates generally were faster than 1 min/m and attained a phenomenal 10 s/m in portions of Cores 144-877A-12R and -13R. This 58-m interval represents a skeletal grainstone (basal Lithologic Subunit IIC) that changes downward into a porous foraminifer skeletal grainstone (Lithologic Subunit IID).

Drilling rates averaged about 1.5 min/m from 150 to 169 mbsf (lower Cores 144-877A-16R through upper -18R) in the lower portion of the skeletal grainstone of Lithologic Subunit IID. Furthermore, they slowed to about 2.5 min/m from 169 to 186 mbsf, reflecting a greater degree of cementation in the lithoclast skeletal foraminifer packstone of Lithologic Subunit IIE. Drilling rates averaged only 9 min/m from 186 to 190 mbsf in the clay-rich basal grainstones and underlying clayey weathering profile (Lithologic Unit III).

At 190 mbsf (1556 m below the present-day sea level), contact was made with a very hard lithology. This level has been interpreted as being the top of weathered basaltic basement.

The seismic reflection profile across the transect through Sites 876 and 877 was inadequate for identifying basement reflectors; therefore, no seismic stratigraphy interpretations are possible.

In summary, the drilling penetration rates at Site 877 on Wodejebato Guyot suggest that the section can be divided into three main parts:

1. A manganese crust overlies 9 m of well-cemented carbonate platform.
2. A 186-m-thick carbonate platform follows. The upper 74 m of this carbonate platform is rudist-rich rudstone interspersed with at least three intervals of well-cemented rudist boundstone. The lower 112 m of the carbonate platform consists of skeletal grainstone to wackestone, which is generally poorly cemented except for the basal 17 m.
3. A volcanic breccia has its upper surface at 190 mbsf, where it is overlain by a 4-m-thick weathering horizon and gradational contact to the overlying carbonate platform.

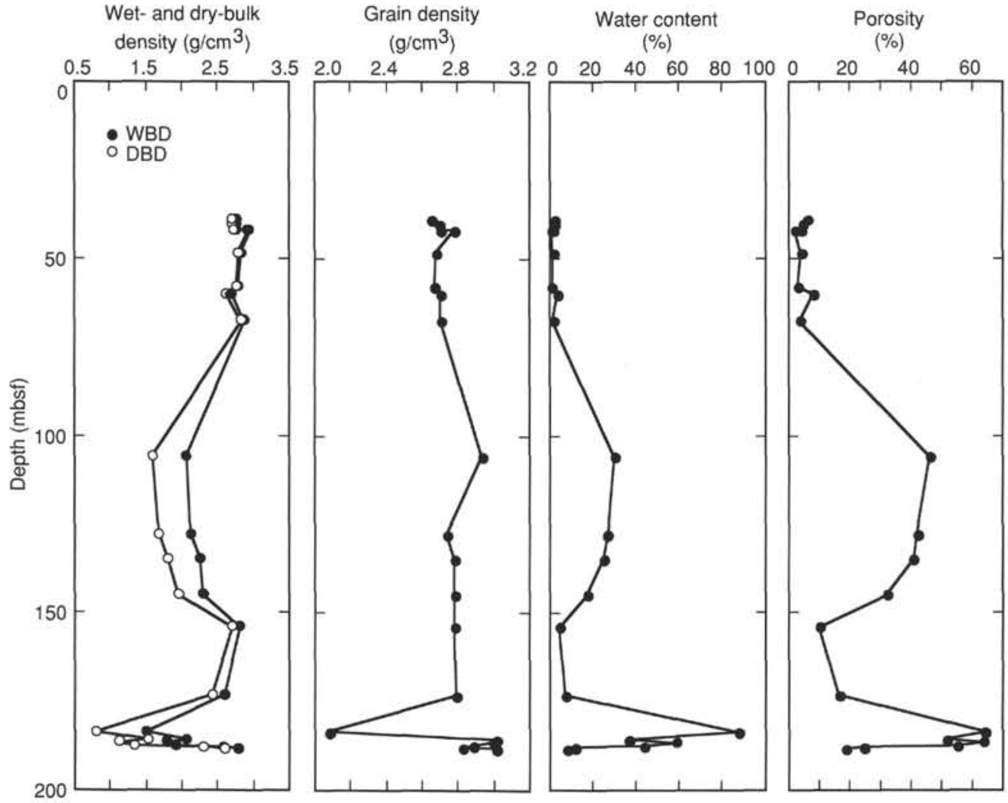


Figure 23. Measurements of index properties (wet- and dry-bulk density, grain density, water content, and porosity) vs. depth, Hole 877A.

## SUMMARY AND CONCLUSIONS

At Site 877, the upper portion of the igneous edifice of Wodejebato Guyot was formed by a volcanic breccia. Overlying the breccia is an in-situ weathering profile of claystone that has retained the fabric of the host volcanic breccia. The presence of root molds, plant remains, and pyrite indicate that the transition from subaerial to marine conditions took place in a low-energy, sulfate-reducing, marine environment. The occurrence of calcareous nannofossils, restricted to the Cenomanian and reworked in the argillaceous limestone, indicates that only the most recent part of the geologic history of Wodejebato Guyot has been recovered at Sites 873–877.

The sedimentation history at Site 877 is similar to that described from Site 874, the twin site farther to the southeast on the inner perimeter ridge. The difference between these two sites is a function of the limestone sequence being 20 m thicker at Site 877 than at Site 874.

At least two bioherms developed at Site 877; these features were also observed at Site 874. At Site 877, the lower, or older, bioherm began with a rudist assemblage dominated by small erect radiolitids. The rudist framework developed from a scattered community of individuals and evolved into clusters of a few individuals. Radiolitids, in life position, are locally encrusted by red algae. Upsection, the rudists become more abundant and form the bulk of the organic framework, whereas red algae diminish in abundance. The assemblage becomes dominated by loosely packed large caprinids, which were typically recumbent and scarcely acquired a gregarious habit. These caprinids formed an open framework that may easily have been smothered by increased sedimentation. This development differs from that recorded at Site 874 in which, in addition to rudists, algae and corals form boundstone. The differences between the assemblages at Sites 874 and 877 suggest a lateral zonation of the bioherm framework in response to their slightly different positions along the axis of the ridge.

The second, more recent episode of bioherm construction is also slightly different between the two sites. At Site 877, algae and caprinid rudists primarily form the boundstone, whereas at Site 874, algae and stromatoporids form the boundstone. At both locations, the framework builders are heavily encrusted by red algae.

As at Site 874, the oldest pelagic sediments recorded at Site 877 are Maastrichtian in age and infill cavities within the upper part of the carbonate platform facies. This association is interpreted as confirming that the production of shallow-water carbonate on Wodejebato terminated before the end of the Cretaceous, either preceded by an emersion episode that generated the cavities or by submarine dissolution that produced the cavities implying only a single drowning event. Pelagic ooze is limited to a thin cover, as observed in the 3.5-kHz profile. The presence of manganese-encrusted, phosphatized lithoclasts of varying origins and ages, which overlie the cavities that contain the pelagic infilling, suggests that Site 877 was a location of prevailing nondeposition. The sequence cored in the upper part of Hole 877A has a similar lithology and age as the hardground recovered at Sites 875 and 876 on the outer perimeter ridge, and at Site 874 on the inner perimeter ridge. This similarity demonstrates that all of Wodejebato Guyot underwent submergence by the late Paleocene. Throughout the Paleogene, current activity inhibited sediment accumulation. By early and middle Eocene times, Wodejebato Guyot was under a zone of high productivity and intensive winnowing; consequently, the manganese-encrusted and phosphatized hardground continued to develop.

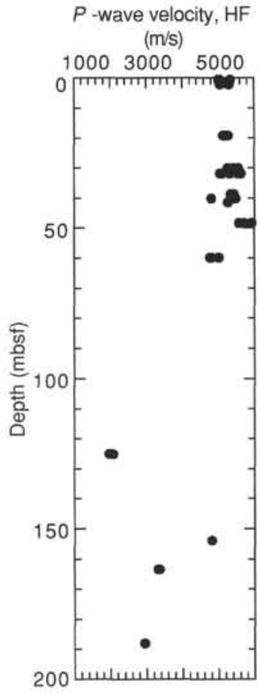


Figure 24. Hamilton Frame (HF) measurements of compressional wave velocity vs. depth, Hole 877A.

## REFERENCES *


Camoin, G., Bernet-Rollande, M.C., and Philip, J., 1988. Rudist-coral frameworks associated with submarine volcanism in the Maastrichtian strata from Pachino area (S.E. Sicily). *Sedimentology,* 23:128–143.

Flügel, E., 1982. *Microfacies Analysis of Limestones:* New York (Springer-Verlag).

Kauffman, E.G., and Sohl, N.F., 1974. Structure and evolution of Antillean Cretaceous rudist frameworks. *Verh. Naturforsch. Ges. Basel,* 84:399–467.

Perch-Nielsen, K., 1985. Cenozoic calcareous nannofossils. *In* Bolli, H.M., Saunders, J.B., and Perch-Nielsen, K. (Eds.), *Plankton Stratigraphy:* Cambridge (Cambridge Univ. Press), 427–554.

Skelton, P.W., 1979. Gregariousness and proto-cooperation in rudists (Bivalvia). *In* Larwood, G., and Rosen, B.R. (Eds.), *Biology and Systematics of Colonial Organisms:* New York (Academic Press), 257–279.

Tebbutt, G.E., Conley, C.D., and Boyd, D.W., 1965. Lithogenesis of a carbonate rock fabric. *Contrib. Geol.,* 4:1–13.

Walker, K.R., and Alberstadt, L.P., 1975. Ecological succession as an aspect of structure in fossil communities. *Paleobiology,* 1:238–257.


* Abbreviations for names of organizations and publication titles in ODP reference lists follow the style given in *Chemical Abstracts Service Source Index* (published by American Chemical Society).

**Ms 144IR-109**

**NOTE: For all sites drilled, core-description forms ("barrel sheets") and core photographs can be found in Section 3, beginning on page 453. Forms containing smear-slide data can be found in Section 4, beginning on page 1017. Thin-section data are given in Section 5, beginning on page 1037.**

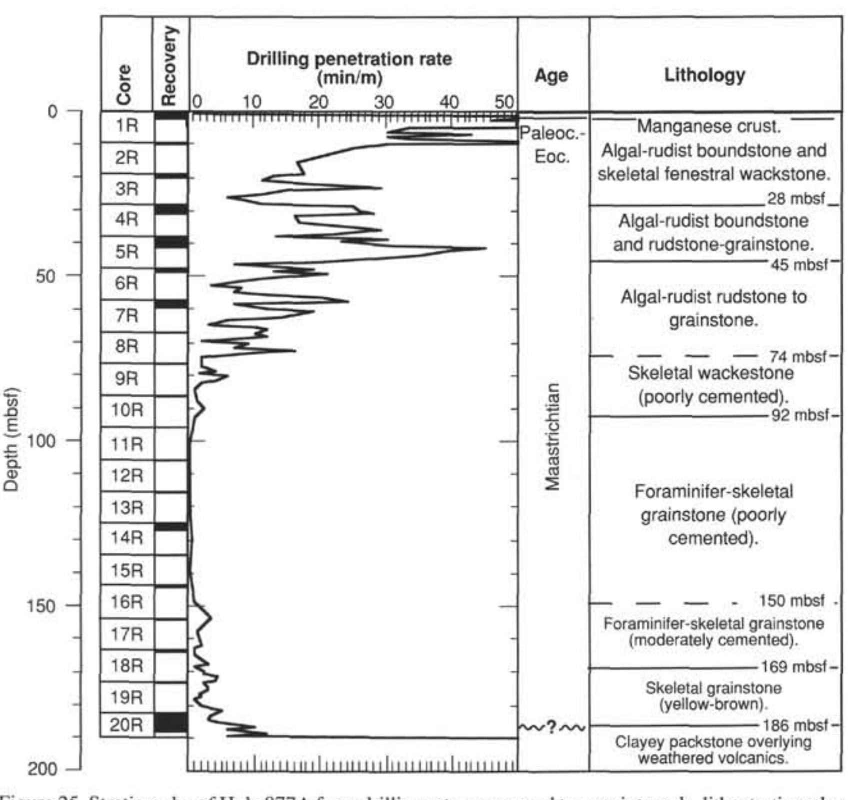


Figure 25. Stratigraphy of Hole 877A from drilling rates compared to core intervals, lithostratigraphy, and biostratigraphic ages within Hole 877A. Drilling rates are plotted as the minutes required to penetrate 1m,. wihch yields a visual display comparable to the resistivity or density logs.